Cannabinoid agonists showing BuChE inhibition as potential therapeutic agents for Alzheimer's disease

ARTICLE *in* EUROPEAN JOURNAL OF MEDICINAL CHEMISTRY · DECEMBER 2013

Impact Factor: 3.45 · DOI: 10.1016/j.ejmech.2013.11.026 · Source: PubMed

European Journal of Medicinal Chemistry 73 (2014) 56–72

Contents lists available at ScienceDirect

European Journal of Medicinal Chemistry

journal homepage: http://www.elsevier.com/locate/ejmech

Original article

Cannabinoid agonists showing BuChE inhibition as potential therapeutic agents for Alzheimer's disease

Pedro González-Naranjo [a], Natalia Pérez-Macias [a], Nuria E. Campillo [a], Concepción Pérez [a], Vicente J. Arán [a], Rocio Girón [b], Eva Sánchez-Robles [b], María Isabel Martín [b], María Gómez-Cañas [c,d,e,f], Moisés García-Arencibia [c,d,e,f], Javier Fernández-Ruiz [c,d,e,f], Juan A. Páez [a,*]

[a] Instituto de Química Médica (CSIC), Juan de la Cierva 3, 28006 Madrid, Spain
[b] Departamento de Farmacología y Nutrición – Unidad Asociada al IQM (CSIC), Facultad de Ciencias de la Salud, Universidad Rey Juan Carlos, Avda. Atenas s/n, 28922 Alcorcón, Spain
[c] Instituto Universitario de Investigación en Neuroquímica, Departamento de Bioquímica y Biología Molecular, Facultad de Medicina, Universidad Complutense, 28040 Madrid, Spain
[d] Centro de Investigación Biomédica en Red sobre Enfermedades Neurodegenerativas (CIBERNED), Universidad Complutense, 28040 Madrid, Spain
[e] Instituto Ramón y Cajal de Investigación Sanitaria (IRYCIS), Universidad Complutense, 28040 Madrid, Spain
[f] CEI-Moncloa UCM – UPM, Universidad Complutense, 28040 Madrid, Spain

ARTICLE INFO

Article history:
Received 31 July 2013
Received in revised form
8 November 2013
Accepted 23 November 2013
Available online 7 December 2013

Keywords:
Alzheimer's disease
Antioxidant
BuChE inhibitor
CB2R agonist
Drug design
Indazole ether
Multitarget drug

ABSTRACT

Designing drugs with a specific multi-target profile is a promising approach against multifactorial illnesses as Alzheimer's disease. In this work, new indazole ethers that possess dual activity as both cannabinoid agonists CB2 and inhibitors of BuChE have been designed by computational methods. On the basis of this knowledge, the synthesis, pharmacological evaluation and docking studies of a new class of indazoles has been performed. Pharmacological evaluation includes radioligand binding assays with [^{3}H]-CP55940 for CB1R and CB2R and functional activity for cannabinoid receptors on isolated tissue. Additionally, *in vitro* inhibitory assays of AChE/BuChE and the corresponding competition studies have been carried out. The results of pharmacological tests have revealed that three of these derivatives behave as CB2 cannabinoid agonists and simultaneously show BuChE inhibition. In particular, compounds **3** and **24** have emerged as promising candidates as novel cannabinoids that inhibit BuChE by a non-competitive or mixed mechanism, respectively. On the other hand, both molecules show antioxidant properties.

1. Introduction

Alzheimer's disease (AD) is a progressive neurodegenerative disorder and is currently the leading cause of dementia in the elderly. Despite of the devastating effects of this disease, therapeutic options for treating AD remain limited. This disease is characterized by the formation of cortical amyloid plaques and neurofibrillary tangles in the brain. A biological function affected in AD is the cholinergic neurotransmission, which seems to be closely related to pathological formation of beta-amyloid. This hypothesis asserts that most of the cognitive impairments suffered by AD patients are the consequence of a deficit in acetylcholine (ACh). In this sense, cholinergic drugs like acetylcholinesterase (AChE) inhibitors, including donepezil, rivastigmine, and galantamine, are currently the most prescribed pharmaceuticals for AD [1–4].

Moreover, Alzheimer's disease is characterized by a significant reduction in AChE activity and an increase in butyrylcholinesterase (BuChE) activity (about 120%). This increase of BuChE activity, especially found in the hippocampus, has been suggested to be related to the loss of episodic memory [5]. Likewise, it has been reported that BuChE might facilitate the transformation of an initial benign form of senile plaque to a malignant form associated with AD [6]. Therefore, the BuChE plays an important role in AD patients, what turns it into an interesting target for the research in the field [5–8].

AChE is characterized by having two sites: a peripheral anionic site (PAS) located at the mouth of the active site gorge, which is regarded as the recognition binding site; and the anionic subsite of

* Corresponding author. Tel.: +34 915622900; fax: +34 915644853.
E-mail addresses: juan@suricata.iqm.csic.es, jpaez@iqm.csic.es (J.A. Páez).

0223-5234/$ – see front matter © 2013 Elsevier Masson SAS. All rights reserved.
http://dx.doi.org/10.1016/j.ejmech.2013.11.026

the active site (CAS), where acetylcholine (ACh)-fixation is occurring before being hydrolyzed in the active site. The interaction with PAS is assumed to be determinant in both the association of AChE with β-amyloid and the formation of amyloid [9–11]. BuChE, also possessing PAS [12,13] and CAS, is present in the neuritic plaques together with AChE. By other hand, BuChE-selective inhibitors have been reported to reduce β-amyloid (AB) and β-amyloid precursor (APP) secretion *in vitro* and *in vivo* [14,15]

New pharmacological alternatives are focused on the development of new drugs capable of acting at different targets [16] (i.e., multitarget drugs) as compounds with anticholinesterase and NMDA receptor antagonistic activity [17]; dual inhibitors of histamine H3 receptors and AChE [18]; dual inhibitors of AChE and BACE1 [19]; dual acting hybrids BACE1 inhibitor and metal chelator [20]; dual acting hybrids gamma-secretase modulators with PPARγ activity [21] or acetylcholinesterase inhibitors and CB1R antagonist [22]. In this context, cannabinoid compounds are very attractive candidates fit to fit into this paradigm since they could act on different pharmacological targets within the so-called endocannabinoid signalling system, but also on other targets not related to this system. It has been reported that the cannabinoid system is dramatically altered in brains of AD patients [23]. Concerning CB1 receptor, the alteration of this receptor is not so clear. In fact, there is some controversy regarding this issue [24]. Some studies suggest that CB1 receptors are intact in AD and may play a role in preserving the cognitive function [25,26], while other studies postulate that the expression and distribution of CB1 are clearly different in AD [27–29]. In any case, it is important to remark the fact that CB1 receptor is located preferentially in damaged neurons in cortical and subcortical areas, which is in accordance to the expected decrease in the levels of this receptor type due to the progressive neuronal loss. Regarding CB2 receptors, different studies show that they are abundantly expressed in neuritic plaque-associated astrocytes and selectively expressed in reactive microglia [30–32] in brains of AD patients, in contrast to their absence or poor expression in these glial cells under healthy conditions. Three potential interventions have been identified using CB2R as target [24]. First, stimulation of CB2 receptors suppresses microglial activation [33,34] second, a CB2 receptor agonist such as JWH-015 is capable of inducing the removal of native beta-amyloid [25,31,35] and third, CB2 receptor agonists suppress the neuroinflammatory process [36]. Taken together, these results suggest that CB1 receptor agonists may interrupt the mechanism of excitotoxicity and CB2 receptor agonists may suppress neuroinflammation and lead to plaque removal.

On the other hand, our group has demonstrated that some cannabinoid agonists such as the aminoalkylindoles (AAI), JWH-015 or WIN 55,212-2 (Fig. 1) inhibit the AChE *in vitro* [37].

Thus, continuing with our effort to develop an efficient strategy to fight against AD and taking advantage of the demonstrated potential of the cannabinoids that are active at both the cholinergic transmission and at the endocannabinoid system, our research group first disclosed a new family of indazole ethers with cholinergic properties and cannabinoid effects showing multitarget drug profile, which opened a novel and interesting therapeutic strategy for AD [38]. Subsequently, a similar approach was published by Rizzo et al. [39]. Herein, we describe the synthesis and biological evaluation of a new family of compounds based on the indazole ether scaffold.

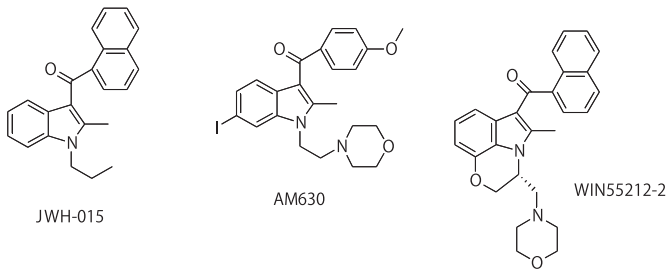

Fig. 1. Chemical structures of representative cannabinoids.

2. Result and discussion

One possible way to find a hit consists of performing systematic modifications of the structure by variation of functional groups at particular sites. In a first approach, three different positions of the indazole system were considered for modulating the biological activity and were subject to modification. Toward this goal, we proposed a procedure that encompassed docking studies of CB2 receptor model [40] and BuChE (pdb code: 1P0I), synthesis and pharmacological evaluation of the effects of structure variations of the indazole system.

2.1. Rational design

Taking into account all above concepts and applying the bioisosterism criterion, we proposed to replace the indole ring by an indazole core, and also introduce an aromatic ether that is well suited for interacting in the binding site of CB2 receptor in a similar way to AAI. Based on the structural superposition of an AAI as JWH-015 with indazole ethers, we designed a virtual library of different indazole derivatives to make a preliminary docking study. For this theoretical study, aimed at evaluating the binding capacity of this new backbone to the receptor, our theoretical model of CB2R* was employed. The virtual library was designed taking account three criteria: i) groups in position 1 and 3 that allow interactions with CB2 receptor, as previously noted in AAI structures; ii) structural variability and iii) synthetic accessibility.

Thus, this initial virtual library was assembled considering as structural variations a hydrogen, or nitro at position 5; benzyl, diisopropylaminoethyl or piperidinoethyl groups at position 1; and benzyl, methoxybenzyl or naphthylmethoxy at position 3 (Fig. 2). Preliminary modelling studies led us to find that several of the virtual compounds showed a favourable energy of interaction compared to the AAI compounds and a similar orientation of the indazole skeleton and the indole ring of AAI.

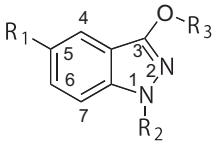

R_1	R_2	R_3
H	$(CH_2)_4CH_3$	$(CH_2)_4CH_3$
NO_2	CH_2-cyclohexyl	CH_2-cyclohexyl
NH_2	$(CH_2)_2$-piperidino	benzyl
Br	$(CH_2)_2$-N-pyrrolidinyl	4-methoxybenzyl
	$(CH_2)_2$-N-$(iPr)_2$	CH_2-1-naphthyl
	$(CH_2)_2$-N-morpholino	CH_2-2-naphthyl
	benzyl	
	4-methoxybenzyl	
	CH_2-1-naphthyl	
	CH_2-2-naphthyl	

Fig. 2. Virtual library. Set of indazole derivatives studied.

On the basis of these modelling results, new substituents were included. Thus, pentyl, cyclohexylmethyl, benzyl, 4-methoxybenzyl, diisopropylaminoethyl, pyrrolidinyl ethyl, morpholinoethyl or piperidinoethyl were considered as substituents at the 1-position of the indazole core. O-Substituted groups as cyclohexylmethyl, benzyl, 4-methoxybenzyl, 1-naphthylmethyl or 2-naphthylmethyl were selected as substituents at position 3 while hydrogen, bromo, nitro or amino were chosen as substituents at position 5 of the indazole ring (Fig. 2).

A docking study was performed using our CB2R model (see details in Computational section), as target against the virtual library. The results of the modelling studies indicated that most of the virtual compounds show favourable energy of interaction and similar orientation of the indazole moiety compared to the indole ring in related AAI, being stabilized by means of an aromatic interaction with Phe197. In addition, the groups in R_2 and R_3 are able to interact with key residues as Leu201 and Tyr190 in TM5 respectively. These initial studies showed that, in general, the N1-substituted derivatives have additional interactions with Met115 and Ser161.

2.2. Chemistry

Based on docking results we performed the synthesis of a representative set of compounds (**1**–**25**) as potential candidates as cannabinoid ligands and ChEs inhibitors (Table 1). As it has been commented in the Introduction, this new family of 1-substituted indazole ethers (**1**–**25**) has been claimed by us in a PCT patent [38]. The synthetic methodology for accessing the target compounds **1**–**25** was based on the introduction of the different groups at N-1 position or at the hydroxyl group of the indazole core through well-established N-alkylation or O-alkylation procedures. Three possible strategies or routes were considered depending on the nature of the desired substituents. The overall synthetic methodology showing the three possible routes is presented in Scheme 1.

The direct base-promoted reaction of the starting indazole core with alkyl halides under refluxing ketone solvent (**route A**) was found to be only useful to obtain disubstituted derivatives with identical groups at both N- and O-positions. For derivatives having different groups at N-1 and OH at C3, **routes B** and **C** were applied. The synthetic **route B** consists of a two-step sequence involving initial alkylation with the a benzylic halide at the more nucleophilic N-1 position of the indazole ethers, and then introduction of the substituent at position 3-OH using different arylmethyl halides. The main limitation of this route is that it proved to be effective only for selective N-alkylation with highly reactive methyl or arylmethyl halides.

A more structurally versatile and general synthetic route for the formation of substituted indazoles, the **route C**, comprises three steps involving protection of position N-1 as a carbamate, O-alkylation to furnish the corresponding ether and subsequent deprotection and introduction of the second substituent at the N-1 position.

Following the **route A**, a wide variety of N-1 substituted indazole ethers were prepared by reaction of indazolol **26** or 5-nitroindazolol **27** [41] with the corresponding halides in acetone or butanone and caesium or potassium carbonate as base (Table 1, Scheme 2). Thus, the synthesis of indazole ethers **1**, **2**, **4**, **8** were carried out starting from **26** and cyclohexylmethyl, benzyl or 4-methoxybenzyl bromides or 1-naphthylmethyl chloride, respectively. Similarly, the 5-nitroindazole ethers **10**, **12** [42] **16**, **21** were

Table 1
Binding affinities (K_i, μM) for CB1 and CB2 receptors of indazole derivatives **1**–**25**.

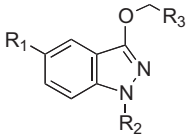

Compd	R_1	R_2	R_3	K_i CB1 (μM)	K_i CB2 (μM)
1	H	CH_2–cyclohexyl	Cyclohexyl	0.2 ± 0.2	1.3 ± 0.6
2	H	CH_2–Ph	Ph	2.6 ± 0.9	3.51 ± 0.09
3	H	$(CH_2)_2$–N–(^{i}Pr)$_2$	4-Methoxyphenyl	>40	7.7 ± 2
4	H	4-Methoxybenzyl	4-Methoxyphenyl	2.4 ± 0.7	0.9 ± 0.2
5	H	$(CH_2)_2$–N–(^{i}Pr)$_2$	1-Naphthyl	>40	5.4 ± 2.6
6	H	$(CH_2)_2$–N–pyrrolidinyl	1-Naphthyl	0.56 ± 0.09	0.4 ± 0.2
7	H	$(CH_2)_2$–piperidino	1-Naphthyl	3 ± 2	0.24 ± 0.05
8	H	CH_2–1-naphthyl	1-Naphthyl	>10	>10
9	H	$(CH_2)_2$–piperidino	2-Naphthyl	1.4 ± 0.5	2 ± 2
10	NO_2	$(CH_2)_4CH_3$	$(CH_2)_3CH_3$	1.3 ± 0.6	0.68 ± 0.04
11	NO_2	CH_2–Ph	Cyclohexyl	>40 (39%)	0.09 ± 0.03
12	NO_2	CH_2–Ph	Ph	1.2 ± 0.3	0.4 ± 0.1
13	NO_2	$(CH_2)_4CH_3$	4-Methoxyphenyl	0.8 ± 0.2	0.49 ± 0.06
14	NO_2	$(CH_2)_2$–N–(^{i}Pr)$_2$	4-Methoxyphenyl	>40	9 ± 2
15	NO_2	$(CH_2)_2$–N–pyrrolidinyl	1-Naphthyl	0.6 ± 0.2	0.13 ± 0.02
16	NO_2	CH_2–1-naphthyl	1-Naphthyl	3.8 ± 0.7	0.24 ± 0.06
17	NO_2	$(CH_2)_4CH_3$	2-Naphthyl	1.6 ± 0.1	1.37 ± 0.06
18	NO_2	$(CH_2)_2$–piperidino	2-Naphthyl	1.3 ± 0.4	0.5 ± 0.1
19	NO_2	$(CH_2)_2$–morpholino	2-Naphthyl	1.38 ± 0.08	0.5 ± 0.2
20	NO_2	CH_2–Ph	2-Naphthyl	>10	0.4 ± 0.2
21	NO_2	CH_2–2-naphthyl	2-Naphthyl	>10	>10
22	NH_2	CH_2–Ph	Ph	4 ± 1	1.6 ± 0.3
23	NH_2	$(CH_2)_2$–N–pyrrolidinyl	1-Naphthyl	11 ± 3	5 ± 2
24	NH_2	$(CH_2)_2$–piperidino	2-Naphthyl	>40	2 ± 1
25	Br	$(CH_2)_2$–piperidino	2-Naphthyl	1.7 ± 0.2	1.8 ± 0.7

Receptors binding studies were performed using membrane fractions of human CB1 or CB2 receptor transfected cells (HEK293EBNA). K_i value of WIN 55,212-2 is 36.2 nM in CB1 receptor. K_i values of WIN 55,212-2 and HU308 are 3.7 and 11.2 nM in CB2, respectively.

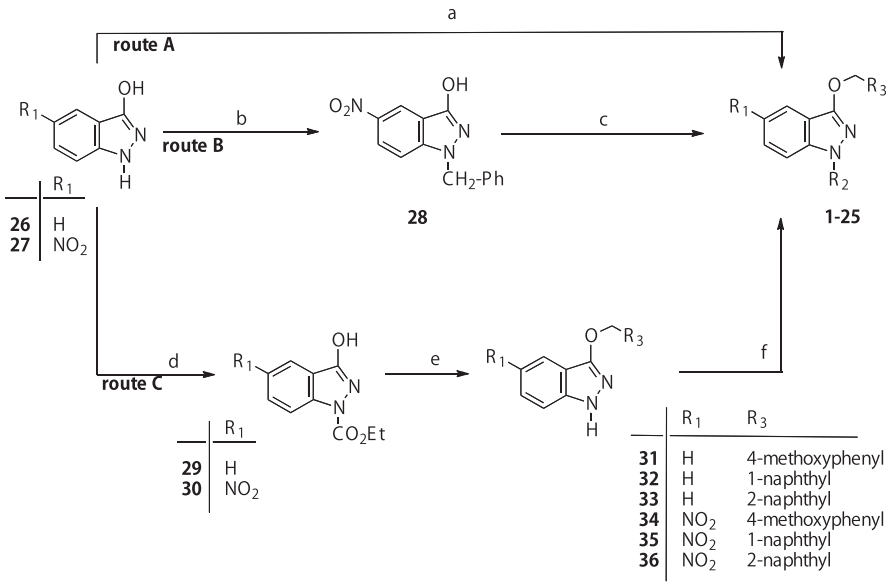

Reagents and conditions: a) $R_2 = R_3$, R_2-X (X=Br, I), K_2CO_3 or Cs_2CO_3, acetone or 2-butanone, reflux; b) benzyl bromide, NaOH, H_2O; c) R_3-Br, K_2CO_3, 2-butanone or Cs_2CO_3, acetone, reflux; d) ClCOOEt, pyridine, rt; e) 1) R_3-X, K_2CO_3, 2-butanone, 1,4-dioxane or DMF, reflux, 2) KOH / EtOH, rt; f) R_2-X, K_2CO_3, 2-butanone, reflux

Scheme 1. Synthetic routes to prepare indazole derivatives.

prepared by reaction of 5-nitro-3-indazolole **27** with the corresponding halides of pentyl, benzyl and 1 or 2-naphthylmethyl, respectively.

The first attempts to synthesize 1,3-disubstituted indazoles with different groups at N-1 position and ether function were carried out following the synthetic **route B** starting from 5-nitroindazolole **27**. Thus, the reaction of **27** with benzyl bromide in an aqueous solution of sodium hydroxide afforded the corresponding 1-benzyl-3-indazolol **28** [43]. Then, subsequent O-alkylation of **28** with cyclohexylmethyl or 2-naphthylmethyl bromide afforded the indazole ethers **11** and **20**.

As mentioned before, the route C was found to be a more versatile and suitable procedure for the sequential two-fold alkylation (at N- and O-centres) with different groups. This strategy resulted especially useful for the preparation of indazole ethers bearing aminoethyl groups at N-1 position. Thus, standard N1-protection of indazoles **26** and **27** with ethyl chloroformiate furnished the corresponding 1-ethoxycarbonyl derivatives **29** [43] and **30** [42], respectively. Next, the reaction of **29** or **30** with the corresponding halides in the presence of K_2CO_3 as base afforded the 5-unsubti tuted derivatives of 4-methoxybenzyloxy **31**, 1-naphthylmethoxy **32**, 2-naphthylmethoxy **33**, or the 5-nitroindazole ethers **34**–**36**, respectively. All reactions were carried out under reflux of butanone, except for derivatives **31** and **35**, where 1,4-dioxane and DMF were, respectively, the solvents of choice. In some cases, migration of the arylmethyl substituent from the O- at C3 to N2 was observed, leading to mixtures of 3-arylmethyloxy-1*H*-indazole and N2-alkylated 1,2-dihydro-3*H*-indazol-3-one derivatives (Scheme 2). For example, the reaction of derivatives **29** and **30** with the corresponding halides yielded a mixture of the corresponding indazole ethers **31**–**36** and their corresponding N-2 substituted derivatives **37**, **38**, **39** [44], **40**, **41**, and **42** [45], respectively. The relative ratio of the two isomers depended on the conditions employed in each case. To the best of our knowledge, there is no reported procedure allowing the selective O-alkylation to afford the ether isomer in good yield. Nevertheless, by tuning the reaction conditions we found conditions to obtain the desired indazole ethers **31**–**36** as the major component of the mixture in all cases, which could be efficiently separated from the mixture by flash chromatography (see Experimental section for detailed conditions).

For the majority of the derivatives, the best results were obtained using 2-butanone as solvent. However, for the preparation of derivative **31** the use of 1,4-dioxane was found to be essential for increasing the ratio of the desired indazole ether over that of the N2-alkylated product. As another exception to this general trend, the synthesis of derivative **35** required harsher reaction conditions and a higher boiling point solvent (DMF). The best O3- versus N2-alkylation ratio was achieved for compounds **32** and **35** for which a relative ratio of 10:1 and 5:1, respectively, was measured by ^{1}H NMR from the crude mixture.

With the 1*H*-indazole **31**–**36** in hand, the last step to obtain the target compounds was the installation of the aminoethyl group at N1 position. The synthesis of 4-methoxybenzyl derivative **3** and 4-methoxybenzyl-5-nitroindazoles **13**, **14** were carried out with

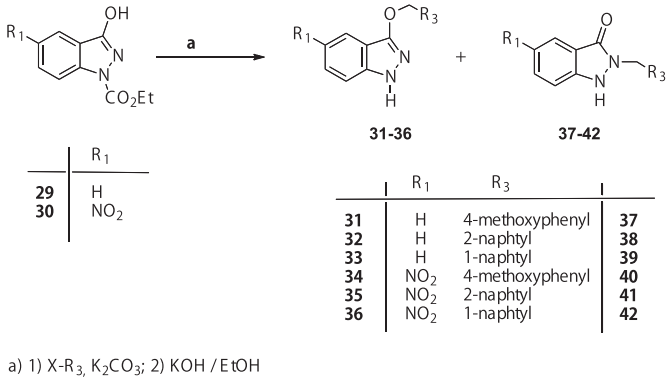

a) 1) X-R_3, K_2CO_3; 2) KOH / EtOH

Scheme 2. Preparation of N-1*H*-indazole ethers.

diisoproylaminoethyl chloride and pentyl iodide, from **31** and **34**, respectively.

The reaction of the 1-naphthylmethoxy indazole **32** with the corresponding aminoethyl chlorides afforded the diisopropylaminoethyl, pyrrolidinyl ethyl and piperidinoethyl derivatives **5**–**7**, respectively. In a similar manner, N-alkylation of the 5-nitro-1-naphthylmethoxy indazole **35** with 2-pyrrolydinnoethyl chloride afforded the corresponding ether **15**. Finally, the preparation of the 3-(2-naphthylmethoxy)indazole derivative was carried out from **33** by N-alkylation with 2-piperidinoethyl chloride to afford the desired derivative **9**.

Similarly, the reaction of the 5-nitro-2-naphthylmethoxy indazole **36** with the corresponding aminoethyl chlorides and alkyl iodides afforded the pentyl, piperidinoethyl and morpholinoethyl ethers **17**–**19**, respectively.

Besides, we have performed novel modifications in the indazole ether system by bromination and reduction reactions (Scheme 3). In this sense, the conversion of the nitro group at C-5 into the corresponding 5-amino derivative had not been reported before. Thus, to the preparation of the 5-amino derivatives **22**–**24** a modification of the standard ferric chloride-promoted procedure was necessary. Following the method describes by Lauwiner et al. [46] for the reduction of monosubstituted nitrobenzenes, the ferric oxyhydroxide FeO(OH) was prepared and used as catalyst by the treatment of $FeCl_3$ with a NaOH solution.

Following this procedure the reaction of the 5-nitro derivatives **12**, **15** and **18** with hydrazine in MeOH in presence of the ferric oxyhydroxide FeO(OH) as catalyst afforded the corresponding 5-amino derivatives **22**–**24**, respectively. The preparation of 5-bromo indazole **25** was achieved by bromination with N-bromosuccinimide and ferric chloride from the 2-naphthylmethoxy-1-piperidinoethylindazole **9**.

The structures of synthesized compounds (**1**–**25**) were established as N1 and O3 disubstituted indazoles on the basis of NMR data (Tables S1 and S2). The position of the 1 and 3 substituents can be distinguished by ^{13}C NMR spectra examining the chemical shifts (Table S2). Thus, the signals corresponding to aromatic methylene group attach at O-3 (66–75 ppm) appears at lower field in relation to methylene N-1 (50–58 ppm). In compounds bearing the methylene groups at N-2 the signals appearing at highest field (45–47.5 ppm).

2.3. Biological assays

2.3.1. In vitro binding studies in cannabinoids receptors

Radioligand displacement assays were used to evaluate the affinity of the new compounds **1**–**25** using membranes from cells (HEK293EBNA) transfected with the CB1 or the CB2 receptors and [^{3}H]-CP55940 as radioligand. Several indazole ethers showed low solubility at concentration greater than 10 μM under test conditions (see Material and methods section), therefore precluding the determination of their quantitative value of IC_{50} for these compounds.

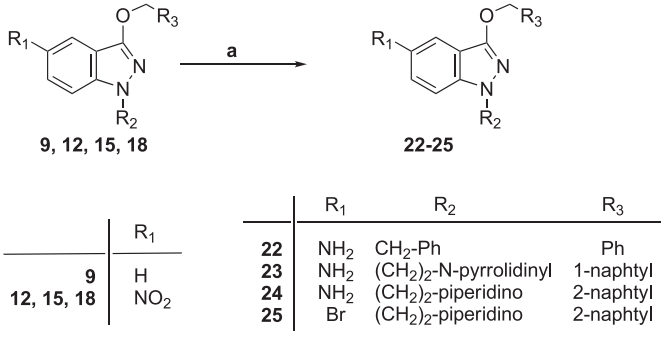

	R_1
9	H
12, 15, 18	NO_2

	R_1	R_2	R_3
22	NH_2	CH_2-Ph	Ph
23	NH_2	$(CH_2)_2$-N-pyrrolidinyl	1-naphtyl
24	NH_2	$(CH_2)_2$-piperidino	2-naphtyl
25	Br	$(CH_2)_2$-piperidino	2-naphtyl

a) R_1 = H: NBS, $FeCl_3$, CH_3CN; R_1=NO_2: H_2N-NH_2, MeOH, FeO(OH)

Scheme 3. Preparation of 5-bromo and 5-aminoindazole ethers.

All synthesized compounds together with their binding affinity for the cannabinoid receptor CB1 and CB2 are gathered in Table 1. Examination of these data indicates that the evaluated derivatives bind to the receptor CB2 in μM range, except the disubstituted naphthyl derivatives **8** and **21**. The comparison of the IC_{50} values for inhibition of CB2R rather flat structure–activity relationships, with values ranging from 0.24 to >10 μM. The situation is less pronounced for CB1 receptor, therefore some of the derivatives such as the diisopropylaminoethyl derivatives **3**, **5**, and **14** do not exhibit affinity to 40 μM. Regarding CB2 selectivity, it is interesting to mark several compounds as the nitro compounds **11**, **16**, **20**, and especially the 5*H*-indazole **7** and the amino derivative **24** due to interesting pharmacological profiles that they will be discussed later.

2.3.2. AChE/BuChE inhibitory activity

The derivatives **1**–**25** were subjected to Ellman's test [47] in order to evaluate their potency to inhibit the AChE from human and BuChE from horse serum and human using donepezil as reference standard. The displayed IC_{50} values in Table 2 showing that several compounds exhibit inhibitory activity of AChE or BuChE at potency levels in the submicromolar to micromolar range. Similarly to the case of cannabinoid binding assays, the quantitative value of IC_{50} for several derivatives was not possible to be determined for solubility reasons Albeit, significant inhibition of AChE, with IC_{50} values in the range of 10 μM, was observed for **5** and **7**.

Regarding AChE inhibition, the results indicate that several indazole derivatives showed significant activity as inhibitors of this enzyme being derivatives **1** and **2** which have lower IC_{50} values among the 5*H*-indazoles.

In relation to BuChE inhibition, several indazole derivatives showing a significative IC_{50} value. The analysis of the IC_{50} values reveals it is necessary but not sufficient, the presence at N1 position of a dialkylaminoethyl group like demonstrated with the 5*H*-indazole derivatives **3**, **5**, **6**, **7**, **9** and with the 5-amino **23**, **24** and 5-bromo **25** compounds. It is interesting to mention that all the other 5*H*-unsubstituted indazole derivatives bearing the aminoethyl group behaved as BuChE inhibitors showing a marked selectivity towards BuChE. In the case of 5-nitroindazole derivatives only the piperidinoethyl **18** and pyrrolidinyl ethyl **15** showed inhibition of BuChE. Noteworthy, these achieved values of inhibitory activity for BuChE are comparable to those published from rivastigmine, a cholinesterase inhibitor used in Alzheimer's disease. The IC_{50} of rivastigmine as AChE or BuChE inhibitor is 1.5–48 μM or 0.3–54 μM respectively, depending on the assay conditions [48–50].

2.3.3. Kinetic study of BuChE/AChE inhibition

To gain further insight into the mechanism of action of this family of compounds, a kinetic study was carried out with the most promising inhibitors of BuChE. Lineweaver–Burk plots were done for the multitarget cannabinoids and donepezil as reference compound and are shown in material supplementary (Figs. S1 and S2) and the data summarized in Table 2. The inhibition constants, K_i, for BuChE inhibitors (Table 2) were determined by fitting the kinetic data to a competitive, noncompetitive, or mixed inhibition model by nonlinear regression analysis using GraphPad Prism 5 [51]. Thus, the competition studies were carried out in all the indazole derivatives with activity as BuChE inhibitors. Albeit deserve special attention those derivatives that behave as cannabinoid agonists and BuChE inhibitors like **3**, **6**, **7**, **9**, **23** and **24** (Table 2).

Table 2
Inhibition of human AChE and human BuChE (IC_{50}, μM) and Oxygen Radical Absorbance Capacity (ORAC, Trolox equivalents) of indazole derivatives and inhibition type of BuChE inhibitors.

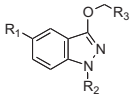

Compd.	R_1	R_2	R_3	IC_{50} AChE[a] human (μM)	IC_{50} BuChE[a] horse (μM)	IC_{50} BuChE[a] human (μM)	k_i[b] BuChE (μM)	k_d BuChE calcd.[c]	BuChE inhibition type[d]	ORAC[e]
1	H	CH_2–cyclohexyl	Cyclohexyl	7.1 ± 0.2	>10	>10	–	–	–	–
2	H	CH_2–Ph	Ph	2.9 ± 1.8	–	>25	–	–	–	–
3	H	$(CH_2)_2$–N–(^{i}Pr)$_2$	4-Methoxyphenyl	>10 (24 ± 2)	2.28 ± 0.04	4.8 ± 0.3	2.6 ± 0.1	0.35	NC	1.0
4	H	4-Methoxybenzyl	4-Methoxyphenyl	>10 (38 ± 6)	>10 (16 ± 2)	>10	–	–	–	–
5	H	$(CH_2)_2$–N–(^{i}Pr)$_2$	1-Naphthyl	>10 (42 ± 3)	–	0.10 ± 0.03	0.028 ± 0.004	2.51	C	–
6	H	$(CH_2)_2$–N–pyrrolidinyl	1-Naphthyl	>10	6.7 ± 0.3	2.83 ± 0.01	1.2 ± 0.3	1.70	C	0.7
7	H	$(CH_2)_2$–piperidino	1-Naphthyl	>10 (46 ± 5)	0.91 ± 0.03	0.81 ± 0.02	0.22 ± 0.03	0.44	C	0.5
8	H	CH_2–1-naphthyl	1-Naphthyl	>10 (40 ± 3)	–	>10	–	–	–	–
9	H	$(CH_2)_2$–piperidino	2-Naphthyl	>10 (15 ± 3)	1.4 ± 0.1	0.97 ± 0.02	1.19 ± 0.06	0.72	NC	0.5
10	NO_2	$(CH_2)_4CH_3$	$(CH_2)_3CH_3$	4.2 ± 0.2	>10	>10	–	–	–	–
11	NO_2	CH_2–Ph	Cyclohexyl	>10 (47 ± 5)	>10 (13 ± 3)	>10	–	–	–	–
12	NO_2	CH_2–Ph	Ph	7.3 ± 0.2	>10 (20.5 ± 0.9)	>10	–	–	–	–
13	NO_2	$(CH_2)_4CH_3$	4-Methoxyphenyl	9.7 ± 0.2	>10	>10	–	–	–	–
14	NO_2	$(CH_2)_2$–N–(^{i}Pr)$_2$	4-Methoxyphenyl	91 ± 2	–	>100	–	–	–	–
15	NO_2	$(CH_2)_2$–N–pyrrolidinyl	1-Naphthyl	>25 (45 ± 3)	–	4.5 ± 1.7	2.1 ± 0.4	0.03	C	–
16	NO_2	CH_2–1-naphthyl	1-Naphthyl	6.7 ± 0.1	–	>10	–	–	–	–
17	NO_2	$(CH_2)_4CH_3$	2-Naphthyl	8.2 ± 0.5	>10	>10	–	–	–	–
18	NO_2	$(CH_2)_2$–piperidino	2-Naphthyl	>10	2.07 ± 0.42	3.6 ± 0.1	2.9 ± 1.4	0.44	M	–
19	NO_2	$(CH_2)_2$–morpholino	2-Naphthyl	>10 (18.2 ± 0.2)	>10 (16 ± 2)	>10	–	–	–	–
20	NO_2	CH_2–Ph	2-Naphthyl	6.3 ± 0.5	>10 (21 ± 3)	>10	–	–	–	–
21	NO_2	CH_2–2-naphthyl	2-Naphthyl	>10 (43 ± 4)	>10	>10	–	–	–	–
22	NH_2	CH_2–Ph	Ph	8.6 ± 0.5	>10 (21 ± 2)	>10 (21 ± 2)	–	–	–	–
23	NH_2	$(CH_2)_2$–N–pyrrolidinyl	1-Naphthyl	>25 (41 ± 3)	–	3.0 ± 0.9	1.0 ± 0.2	0.31	C	1.3
24	NH_2	$(CH_2)_2$–piperidino	2-Naphthyl	>10 (13 ± 4)	1.5 ± 0.1	1.78 ± 0.01	0.38 ± 0.06	0.54	M	0.8
25	Br	$(CH_2)_2$–piperidino	2-Naphthyl	>10	–	0.19 ± 0.01	0.079 ± 0.008	0.51	C	–
		Donepezil		10 ± 2 nM	2.50 ± 0.07	–				–
		Rivastigmine		1.54 ± 0.06	–	0.30 ± 0.01				–

[a] IC_{50} values (mean ± SEM) were determined from 3 different experiments using acetylthiocholine and butyrylthiocholine (0.8 and 0.5 mM, respectively) as substrates.
[b] k_i values (mean ± SEM) were determined from 3 different experiments using combinations of four substrate concentrations, and three inhibitor concentrations.
[c] k_d values were calculated using STC program.
[d] BuChE inhibition type, M: mixed, C: competitive, NC: non-competitive.
[e] Data are expressed as μmol of Trolox equivalents/μmol of tested compound.

Reciprocal plot for donepezil inhibition showed both increasing slopes (decreased at increasing inhibitor concentrations) and increasing intercepts with higher inhibitor concentration (Fig. S1). These results indicate a mixed-type inhibition and are in agreement with patterns obtained with the same enzyme [52]. Therefore, kinetic studies suggested two potential different site of interaction: the active site and the peripheral binding site.

Regarding the inhibition type of BuChE, compounds **18** and **24** (Fig. S2) showed similar plots to donepezil pointing to a mixed type competitive BuChE inhibition mode of action. Lineweaver–Burk plots obtained for **5**, **6**, **7**, **15**, **23** and **25** (Fig. S2) increase in the slope at increasing inhibitor concentrations, typical for a pure competitive BuChE inhibitor. Reciprocal plot for **3** and **9** (Fig. S2) showed unvaried y-intercepts and increasing slopes at increasing inhibitor concentrations compatible with non-competitive BuChE inhibitors.

Moreover, complementary competition studies in AChE were performed with the indazole derivatives inhibitors of BuChE that showed an IC_{50} about 10 μM as AChE inhibitors like **5** and **7**. In a similar way to BuChE, the analysis of the graphic profiles of **5** and **7** (Fig. S3) can be established that **5** and **7** showed a competitive mode of action as AChE inhibitors.

2.3.4. Cannabinoid activity. Isolated tissue assays

According to the objectives, all derivatives that showed simultaneously activity as cannabinoid ligands and as inhibitors of BuChE have been studied in detail in isolated tissues. The functional activity of the new compounds **3**, **5**–**7**, **9**, **15**, **18** and **23**–**25** has been tested on mouse vas deferens (MVD) a tissue commonly used to study and characterize cannabinoid effects [53,54]. In MVD cannabinoid agonists, acting at prejunctional cannabinoid receptors, reduce ATP and noradrenaline release and inhibit the electrically evoked smooth muscle contractions. In this tissue, cannabinoid receptor antagonists oppose the inhibitory effect of agonists in a competitive and surmountable manner. CB1 and CB2-like cannabinoid receptors seem to be involved in this effect [55,56].

From the tested compounds, at the used concentrations (10^{-7}–2×10^{-5} M), some derivatives were able to significantly modify the electrically induced contractile response. As Fig. 3 shows, compounds **3**, **6**, **7**, **9**, **15** and **23**–**24** induced a concentration-dependent inhibition of the electrically evoked contractions; from these data, it could be established that these compounds behave as agonists. Furthermore, the effectiveness (maximum effect) of **6**, **7**, **9** and **23**–**24** was similar to that of the reference cannabinoid agonist WIN 55,212-2.

Considering that compounds **3**, **6**, **7**, **9**, **15**, **23** and **24** showed an interesting profile as potential cannabinoid agonists, the blockade of their effect by the CB1 and CB2 receptors antagonists were tested, alone (AM251) or in combination (AM251 + AM630). These drugs were added to the organ bath before each concentration of the new compounds (10^{-7}–2×10^{-5} M).

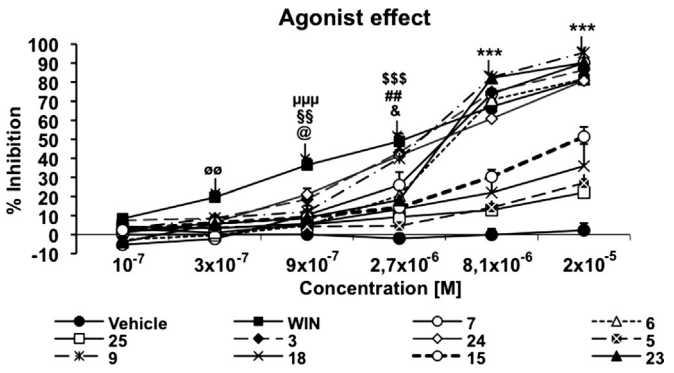

Fig. 3. Effect of WIN 55,212-2 (WIN) and compounds **3**, **5**–**7**, **9**, **15**, **18** and **23**–**25** in mouse vas deferens (MVD). Lines show the means% ± S.E.M. ($n = 6$–8) of inhibition of the electrically induced contraction of the MVD by addition of increasing concentrations of vehicle (Control), WIN or the new compounds. The symbols above the arrows represent the significant difference versus vehicle: $^{***}p < 0.001$: WIN, **3**, **6**, **7**, **9**, **15**, **23** and **24**; $^{\$\$\$}p < 0.001$: WIN, **3**, **7**, **9** and **24**; $^{\#\#}p < 0.01$: **6** and **23**; $^{\&}p < 0.05$: **15**; $^{\mu\mu\mu}p<0.001$: WIN; $^{\S\S}p < 0.01$: **9**; $^{@}p < 0.05$: **24**; $^{øø}p<0.01$: WIN (Two-ways ANOVA, Bonferroni's post-hoc test).

Results showed a partial blockade of the effect of the new derivatives **3**, **9** and **24** that was maximum at the concentration of 2.7×10^{-6} M (Fig. 4A), indicating that their mechanism of action includes the activation of the cannabinoid receptors CB1/CB2

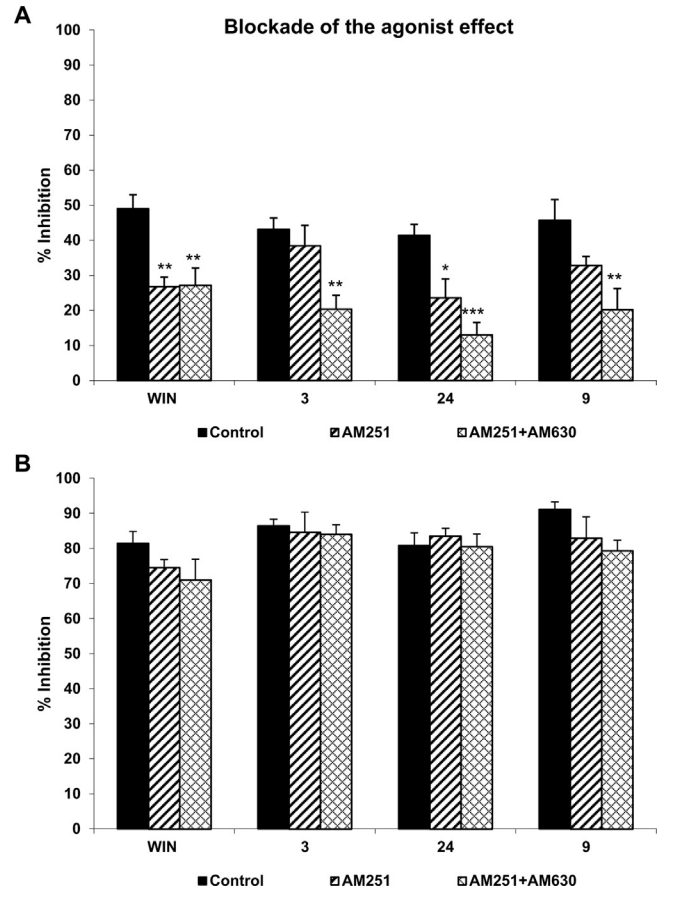

Fig. 4. Bars show the inhibitory effect of the electrically evoked contractions of MVD induced by WIN 55, 212-2 (WIN) or the new compounds **3**, **9** and **24** (A: effect at 2.7×10^{-6} M, B: effect at 2×10^{-5} M) in control preparations (black bars) and in those pretreated with AM251 (10^{-6} M) (striped bars) or AM251 (10^{-6} M) + AM630 (10^{-6} M) (checked bars). *Represents the significant difference versus control: $^{***}p < 0.001$, $^{**}p < 0.01$, $^{*}p < 0.05$ (One-way ANOVA, Bonferroni's post-hoc test).

confirming our hypothesis. The lack of antagonist efficacy on the inhibition induced by the highest concentration of the new compounds (2×10^{-5} M) suggests a surmountable antagonism, perhaps competitive (Fig. 4B).

Compounds **3**, **9** and **24** had the better profile as cannabinoid agonists because they inhibited in a concentration-dependent manner the electrically evoked contractions on mouse vas deferens and this effect was significantly blocked by CB1 and CB2 receptor antagonists.

The inhibitory effects of the MVD contraction of compounds **6**, **7** and **23** are not modified by the presence in the organ bath of the cannabinoid antagonists, so they can be due to other mechanisms that not involve cannabinoid receptors and that are not the object of study in this experimental work.

Taking in consideration our present aim, compounds **5**, **15**, **18** and **25** did not show an interesting profile because their inhibitory effect is too slight.

2.3.5. Antioxidant activity

The antioxidant activities of indazole ether derivatives **3**, **6**, **7**, **9**, **23** and **24** were evaluated by following the well-established ORAC-FL method (oxygen radical absorbance capacity by fluorescence) [57,58]. The results shown in Table 2 indicate that indazole ether derivatives exhibit antioxidant properties with values higher than 45% in relation to Trolox. The 5-aminoindazole derivatives **23** and **24** protect much more efficiently against free radicals (about to thirty percent) than the corresponding 5*H*-indazoles **6** and **9**, respectively.

In summary, the obtained results about indazole ethers derivatives that possess simultaneously activity as cannabinoid agonists and as inhibitors of BuChE showed certain antioxidant capacity, in particular for the noncompetitive **3** and competitive inhibitor of BuChE **23**. This last compound showed the most antioxidant capacity about 29% higher than Trolox.

2.4. Computational studies

To rationalize the achieved biological properties for all derivatives that showed simultaneously activity as cannabinoid agonists and as inhibitors of BuChE docking studies have been carried out employing both targets, CB2R and BuChE. These simulations were attained employing FlexiDock module of the SYBYL 7.2 suite of programs [59].

2.4.1. CB2R-ligands complexes

In our group we have been working on modelling the cannabinoid receptors for several years [40,60]. The first models in the inactive form were built with the pattern of bovine rhodopsin (pdb code: 1f88 [61]). Later, we have modelled CB2 receptor in the active form (results not published). The docking and scoring runs were performed using FlexiDock program [59]. Fig. S4 allows us to verify that our indazole derivatives occupy a similar area that the known agonist JWH-015, showing similar interactions with the residues of the binding site [62] (see Supplementary material, Table S3). The results of the docking experiments for the compounds **3**, **5**–**7**, **9**, **15**, **18** and **23**–25 in CB2R* model in terms of key interactions are gathered in Table S3. The most important difference is the displacement of the naphthyl group due to the replacement of carbonyl group by the ether function. Probably, this displacement is translated in a weak aromatic interaction with Phe197 and Trp258. Observing the Fig. S4, this displacement is a bit more noticeable in the 2-naphthyl derivatives. Further discussion of the docking studies with CB2R model is found in Supplementary material.

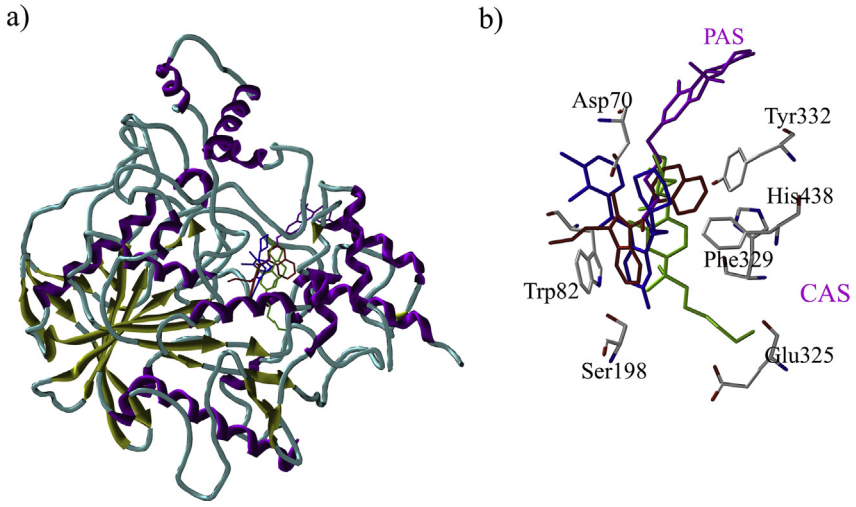

Fig. 5. Schematic representation of BuChE. a) Ribbon diagram of BuChE highlights the residues of the binding site. b) Zoom of the binding site.

2.4.2. BuChE-ligands complexes

Regarding the recognition partners between the ChEs and the cannabinoid ligands, docking simulations were done in the 3D structure of human AChE and BuChE (PDB codes: 1B41 [63] and 1P0I [64], respectively). The interaction modes of active ChE inhibitors in AChE or BuChE were studied employing FlexiDock program [59] (see Experimental section for details). The binding gorge of AChE, which is composed of the central catalytic pocket (CAS) and the peripheral site (PAS), was taken as the binding site for docking studies. For each inhibitor, conformation with the lowest interaction energy was taken out for further analysis. In a previous work we studied an example of each known binding mode: donepezil (mixed), propidium (no-competitive) and edrophonium (competitive) in order to test our docking protocol with good results [37]. Using the same methodology, BuChE inhibitors **3**, **5**–**7**, **9**, **15**, **18** and **23**–**25** were studied and the k_d values were calculated with STC program [65] (Table 2). Highlight that the predicted k_d values are in agreement to the experimental inhibition constants k_i as shown in the Fig. S5 (see Supplementary material).

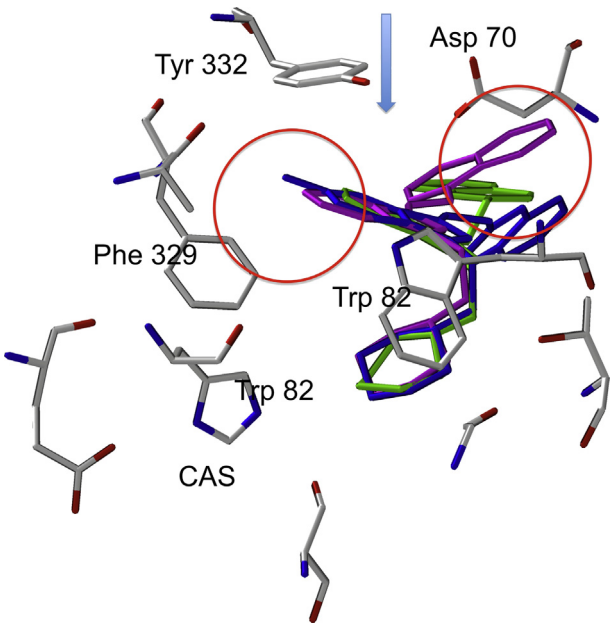

Fig. 6. Structural superposition of an example of each type of inhibition. The competitive example is shown in magenta colour. The non-competitive example is shown in blue colour. The mixed example is shown in green colour. (For interpretation of the references to colour in this figure legend, the reader is referred to the web version of this article.)

The best docking solutions of the most interesting compounds **3**, **6**, **7**, **9**, **15**, **23** and **24** clearly show that these derivatives are located along the tunnel between the sites of the PAS and CAS BuChE (Fig. 5, Table S4). Visually, it is observed that indazole derivatives orientate the group indazole of the position in N1 towards the interior of the channel, so that the indazole group is closed to Trp82. Another interesting observation is regarding to the existence of two clusters of inhibitors due to the different group in R_3 and therefore different orientation of the group, driven the kinetic of the inhibition. Thus, one of the cluster, it is formed by compounds **7**, **6**, and **23** (1-naphthyl substituent on R_3) behaving as competitive inhibitors and the second cluster, it is formed by compound **3** (1-methoxyphenyl on R_3) and **9** and **24** (2-naphthyl substituent on R_3) behaving as non-competitive.

The group at R_3 could be driving the type of inhibition since the 1-naphthyl derivatives behave as competitive inhibitors meanwhile the 2-naphthyl derivatives as non-competitive-mixed inhibitors (Fig. 6). This fact could be due to a relocation of the 2-naphthyl group to avoid a steric hindrance of the 2-napthyl ring with Thr284 and Pro285. Thanks to this movement of the ring, two other interactions appear, one of them with Thr120 (by hydrogen bond with the indazole nitrogen) and the other one with Ser287 (π-HB with 2-naphthyl) (Fig. S6) and unlocking the entrance of the triad catalytic. Further discussion of the interactions of the most representative compounds is displayed in the Supplementary material.

3. Conclusions

On the basis of this investigation, a novel and plausible approach based on the discovery of CB2 cannabinoid agonists that behave as BuChE inhibitors is proposed. Docking techniques have been effectively used to design new cannabinoids derivatives with an innovative indazole ether structure. Remarkably, more than 90% of evaluated compounds have shown capacity to bind CB2 cannabinoid receptor. Among them, according to tissue studies, compounds **3**, **6**, **7**, **9**, **23** and **24** behave as agonists showing a maximum effect similar to the reference cannabinoid agonist WIN 55,212-2. The AChE and BuChE inhibition studies show that these

cannabinoids (**3**, **6**, **7**, **9**, **23** and **24**) are inhibitors of BuChE with comparable values to rivastigmine.

The kinetic and modelling studies have provided insights into the mode of action and the binding site of these compounds. The full agonists **3** and **9** showed a non-competitive inhibition mode, while **24** showed a mixed type inhibition mode of action. Moreover, the BuChE inhibitors **6**, **7** and **23** showed a competitive inhibition mode of action. It is worth mentioning that the indazole derivative **7** inhibits AChE with a mixed action mode. However, in despite of this different behaviour, the docking studies of indazole derivatives in BuChE have allowed the identification of the amino acids involved in the binding site, suggesting that the six indazole derivatives **3**, **6**, **7**, **9**, **23** and **24** are located along the tunnel from PAS to CAS interacting with different residues of peripheral site. Derivatives, **3**, **9**, **24** behave as full agonist cannabinoids according to their capacity to block the agonist effect caused by cannabinoids antagonists as AM251 and AM630. On the other hand, compounds **3**, **24**, and **23** showed the most interesting antioxidant properties.

In summary, the cannabinoid effect, the inhibition of the BuChE of compounds **3** (noncompetitive inhibition type) and **24** (mixed inhibition type) along with its antioxidant capacity suggest that these compounds can be regarded as a potential agent useful for Alzheimer's disease.

4. Experimental section

4.1. Chemistry

4.1.1. General

Melting points were determined with a Reichert-Jung Thermovar micro melting point apparatus and are uncorrected. ^{1}H NMR spectra (300 MHz, DMSO-d_6) and ^{13}C NMR spectra (75 MHz) were recorded on a Gemini or Varian XL-300 (Varian Unity 300 and 400 Varian Gemini and Bruker Avance 300 spectrometers) and are reported in ppm. The signal of the solvent was used as reference. Mass spectra (electrospray ionization) were determined on a MSD-Serie 1100 Hewlett Packard instrument. Elemental analyses were performed on a Heraeus CHN–O Rapid Analysis in our Analytical Services at Centro de Química Orgánica "Manuel Lora Tamayo" (CSIC). Flash column chromatography was carried out using Merck silica gel 60 (230–400 mesh). HPLC-EMS was performed on an Sunfire C_{18} (4.6 × 50 mm, 3.5 mM) column at 30 °C, with a flow rate of 0.25 mL/min. with different gradients of CH_3CN with 0.08% of formic acid (solvent A) in 0.1% of formic acid in H_2O (solvent B) were used as mobile phases. The initial conditions, time of gradient (gt) and time of retention (rt) are specified in each case. The HPLC system was a Waters 2695 Separations Module coupled to a Waters 2996 Photodiode Array detector and to a Waters micromass ZQ. The purity of all compounds was >95% prior to biological testing (Supplementary material).

All starting materials were commercially available in Aldrich or Alfa Aesar and used without further purification. 5-Nitro-3-indazol-ol (**27**) was prepared from the procedure reported by Pfannstiel [41], 1-benzyl-3-bencyloxy-5-nitroindazole (**12**) and 1-ethoxycarbonyl-3-indazolone (**30**) were prepared from the procedure reported by Arán [42], 1-benzyl-5-nitro-3-indazolone (**28**) and 1-ethoxycarbonyl-3-indazolone (**29**) were prepared from the procedure reported by Palazzo [43].

4.1.2. General procedure for the synthesis of indazole ethers 1-substituted ***1***, ***2***, ***4***, ***8***, ***10***, ***16***, ***21*** ($R_2 = R_3$). Method A

The corresponding halide was added to a suspension of the 1*H*-3-indazolol derivative in acetone and Cs_2CO_3. The reaction mixture was refluxed, filtered and evaporated to dryness. The residue was purified by silica gel column chromatography using a mixture of dichloromethane:hexane (1:1, 5:1) as eluent.

4.1.3. General procedure for the synthesis of indazole ethers 1-substituted ***3***, ***5–7***, ***9***, ***13–15***, ***17–19*** from 1H-indazole ethers. Method B

A suspension of the 1*H*-3-indazolol derivative in butanone and K_2CO_3 was treated with the corresponding halide. The reaction mixture was refluxed, filtered and evaporated to dryness. The residue was recrystallized or purified by silica gel column chromatography using the appropriate eluent.

4.1.4. General procedure for the synthesis of indazole ethers ***11*** and ***20*** from N1-substituted indazolol derivative ***28***. Method C

A suspension of **28** in butanone and K_2CO_3 or acetone and Cs_2CO_3 was treated with the corresponding halide. The reaction mixture was refluxed, filtered and evaporated to dryness. The residue was purified by silica gel column chromatography for **11** and recrystallized for **20**.

4.1.5. General procedure for the synthesis of 5-aminoindazoles ***22–24*** from 5-nitroindazoles. Method D

To a suspension of the corresponding 5-nitroindazole 1*H*-3-indazolol derivative in methanol and the modified catalyst FeO(OH) under argon atmosphere, monohydrated hydrazine in excess was added. The reaction mixture was achieved at 50–70 °C for 24–30 h. Then, the suspension was filtered with Zelite and the solvent evaporated to dryness. The residue was treated with water and chloroform and the organic layers evaporated to dryness yielding the corresponding indazole as red oil.

4.1.6. General procedure for the synthesis of indazoles ***31–42*** from 1-ethoxycarbonyl derivatives. Method E

The corresponding halide was added to a suspension of the 1-ethoxycarbonyl-3-indazolol derivative in acetone, K_2CO_3 and catalytic amount of KI. The reaction mixture was refluxed until the end of reaction. The reaction mixture was evaporated to dryness and the residue was treated with water and chloroform. The organic layers were evaporated to dryness and a solution of 0.4 M KOH and ethanol were added. The solution was stirred at room temperature for 1 h and them evaporated to dryness and the residue was purified by silica gel column chromatography using as eluent a mixture chloroform/methanol (100:0, 80:1, 50:1).

4.1.7. 3-(Cyclohexylmethoxy)-1-(cyclohexylmethyl)indazole (***1***)

Following the procedure A, from **26** (0.41 g, 3.01 mmol), cyclohexylmethyl bromide (1.20 mL, 8.67 mmol) and K_2CO_3 (0.86 g, 6.20 mmol) in acetone (60 mL). Reaction time: 48 h. Yield: (0.10 g, 10%). Oil. ^{1}H NMR (300 MHz, DMSO-d_6) δ: 7.52 (d, 1H, 4-H); 7.44 (d, 1H, 7-H); 7.30 (t, 1H, 5-H); 6.95 (t, 1H, 6-H); 4.06 (d, 2H, O–CH_2); 3.98 (d, 2H, N1–CH_2); 1.8–0.9 (m, 22H, 2Cy). ^{13}C NMR (300 MHz, DMSO-d_6) δ: 154.8 (C-3); 141.4 (C-7a); 127.0 (C-6); 119.2 (C-5); 118.7 (C-4), 111.5 (C-3a), 109.4 (C-7); 73.9 (O–CH_2); 53.9 (N1–CH_2); 38.3 (CH); 37.0 (CH); 30.1 (2C, CH_2); 29.2 (2C, CH_2); 26.0 (2C, CH_2); 25.9 (2C, CH_2); 25.3 (CH_2); 25.2 (CH_2). HPLC-MS (ES^+): CH_3CN/H_2O 10:90, gt: 6 min; rt: 6.15, $M + H]^+ = 327.4$.

4.1.8. 1-Benzyl-3-benzyloxyindazole (***2***)

Following the procedure A, from **26** (0.05 g, 0.38 mmol) (Alfa-Aesar), benzyl bromide (0.215 mL, 0.90 mmol) and Cs_2CO_3 (0.51 g, 1.56 mmol) in acetone (60 mL). Reaction time: 48 h. Yield: (0.74 g, 62%). Oil. ^{1}H NMR (300 MHz, $CDCl_3$) δ: 7.76 (d, 1H, 4-H); 7.61–7.23 (m, 10H, 2Bn); 7.43 (d, 1H, 7-H); 7.39 (t, 1H, 5-H); 7.10 (t, 1H, 6-H); 5.52 (d, 2H, O–CH_2); 5.48 (d, 2H, N1–CH_2); ^{13}C NMR (300 MHz, $CDCl_3$) δ: 156.3 (C-3); 142.1 (C-7a); 128.4 (C-6); 120.7 (C-5); 119.7

(C-4); 113.6 (C-3a); 109.3 (C-7); 71.2 (O–C); 52.8 (N1–C); 137.9 (Ar); 137.5 (C, Ar); 129.0 (2C, Ar); 128.9 (2C, Ar); 128.6 (2C, Ar); 127.9 (2C, Ar); 127.5 (2C, Ar). HPLC-MS (ES^+): CH_3CN/H_2O 50:95, gt: 6 min; rt: 5.41, $[M + H]^+ = 315.1$.

4.1.9. 1-(2-Diisopropylaminoethyl)-3-(4-methoxybenzyloxy) indazole (**3**)

Following the procedure B, from **31** (0.19 g, 0.80 mmol), 2-diisopropylaminoethyl chloride hydrochloride (0.16 g, 0.80 mmol) and K_2CO_3 (0.62 g, 4.49 mmol) in 2-butanone (60 mL). The final product was purified by chromatography column using as eluent dichloromethane:methanol (1:0, 30:1). Reaction time: 60 h. Yield: (0.10 g, 33%). Oil. ^1H NMR (300 MHz, $CDCl_3$) δ: 7.63 (d, 1H, 4-H); 7.47 (d, 2H, Ar); 7.45 (d, 1H, 7-H); 7.32 (t, 1H, 5-H); 6.99 (t, 1H, 6-H); 6.92 (d, 2H, Ar); 5.36 (s, 2H, O–CH_2); 4.16 (t, 2H, N1–CH_2); 3.01 (m, 2H, CH); 2.81 (t, 2H, CH_2); 0.98 (d, 12H, CH_3). ^{13}C NMR (300 MHz, $CDCl_3$) δ: 159.5 (Ar); 155.6 (C-3); 141.7 (C-7a); 130.0 (2C, Ar); 129.8 (2C, Ar); 129.4 (C, Ar); 126.9 (C-6); 120.0 (C-5); 118.6 (C-4); 113.8 (2C, Ar); 112.4 (C-3a); 108.8 (C-7); 70.4 (O–CH_2); 55.3 (O–CH_3); 50.5 (2C, CH); 48.9 (N1–CH_2); 44.9 (CH_2); 20.8 (4C, CH_3). HPLC-MS (ES^+): CH_3CN/H_2O 10:90, gt: 6 min; rt: 2.94, $[M + H]^+ = 179.7$.

4.1.10. 1-(4-Methoxybenzyl)-3-(4-methoxybenzyloxy)indazole (**4**)

Following the procedure A, from **26** (0.40 g, 2.94 mmol), 4-methoxybenzyl chloride (0.95 mL, 7.00 mmol) and Cs_2CO_3 (1.95 g, 6.00 mmol) in acetone (40 mL). Reaction time: 48 h. Yield: (0.68 g, 60%). Oil. ^1H NMR (300 MHz, DMSO-d_6) δ: 7.65 (dd, 1H, 4-H); 7.45 (d, 2H, Ar); 7.30 (t, 1H, 5-H); 7.17 (dd, 1H, 7-H); 7.13 (d, 2H, Ar); 7.01 (t, 1H, 6-H); 6.91 (d, 2H, Ar); 6.81 (d, 2H, Ar); 5.36 (s, 2H, O–CH_2); 5.34 (s, 2H, N1–CH_2); 3.82 (s, 3H, O–CH_3); 3.77 (s, 3H, O–CH_3). ^{13}C NMR (300 MHz, DMSO-d_6) δ: 159.9 (C–OCH_3); 159.4 (C–OCH_3); 156.2 (C-3); 141.9 (C-7a); 129.9 (2C, Ar); 129.6 (Ar); 129.2 (Ar); 128.4 (2C, Ar); 127.2 (C-6); 120.1 (C-5); 119.0 (C-4); 113.9 (2C, Ar); 113.8 (2C, Ar); 113.2 (C-3a); 108.8 (C-7); 70.4 (O–CH_2); 55.3 (O–CH_3); 55.2 (O–CH_3); 51.9 (N1–CH_2). HPLC-MS (ES^+): CH_3CN/H_2O 20:100, gt: 20 min; rt: 15.18, $[M + H]^+ = 375.14$.

4.1.11. 1-(2-Diisopropylaminoethyl)-3-(1-naphthylmethoxy)-indazole (**5**)

Following the procedure B, from **32** (0.15 g, 0.54 mmol), 2-diisopropylaminoethyl chloride hydrochloride (0.33 g, 2.42 mmol) and K_2CO_3 (0.39 g, 2.82 mmol) in 2-butanone (60 mL). The final product was purified by chromatography column using as eluent dichloromethane:methanol (1:0, 30:1). Reaction time: 24 h. Yield: (0.069 g, 32%). Oil. ^1H NMR (300 MHz, $CDCl_3$) δ: 7.72 (dd, 1H, 4-H); 7.60 (dd, 1H, 7-H); 7.33 (t, 1H, 5-H); 8.21 (t, 1H, 6-H); 7.91–7.40 (m, 7H, Ar); 5.88 (s, 2H, O–CH_2); 4.20 (t, 2H, N1–CH_2); 3.02 (t, 2H, CH_2); 2.85 (t, 2H, CH); 0.99 (d, 12H, CH_3). ^{13}C NMR (300 MHz, $CDCl_3$) δ: 155.6 (C-3); 141.7 (C-7a); 127.0 (C-6); 120.0 (C-5); 118.7 (C-4); 112.4 (C-3a); 108.8 (C-7); 69.1 (O–CH_2); 50.2 (2C, CH); 49.2 (N1–CH_2); 44.9 (CH_2); 20.8 (4C, CH_3); 133.8 (C, Ar); 132.8 (C, Ar); 131.9 (C, Ar); 129.0 (C, Ar); 128.6 (C, Ar); 127.2 (C, Ar); 126.3 (C, Ar); 125.8 (C, Ar); 125.3 (C, Ar); 124.1 (C, Ar). HPLC-MS (ES^+): CH_3CN/H_2O 10:100, gt: 6 min; rt: 3.66, $[M + H]^+ = 402.2$.

4.1.12. 3-(1-Naphthylmethoxy)-1-(2-(pyrrolidin-1-yl)ethyl) indazole (**6**)

Following the procedure B, from **32** (0.20 g, 0.74 mmol), 2-pyrrolydinoethyl chloride hydrochloride (0.14 g, 0.79 mmol) and K_2CO_3 (3.90 g, 2.82 mmol) in 2-butanone (60 mL). The final product was purified by chromatography column using as eluent dichloromethane:methanol (1:0, 30:1). Reaction time: 60 h. Yield: (0.21 g, 75%). Oil. ^1H NMR (300 MHz, $CDCl_3$) δ: 7.71 (dd, 1H, 4-H); 7.47 (dd, 1H, 7-H); 7.36 (t, 1H, 5-H); 7.00 (t, 1H, 6-H); 7.91–7.40 (m, 7H, Ar); 5.87 (s, 2H, O–CH_2); 4.44 (t, 2H, N1–CH_2); 3.05 (t, 2H, CH_2); 2.63 (d, 4H, CH_2); 1.80 (d, 4H, CH_2). ^{13}C NMR (300 MHz, $CDCl_3$) δ: 155.8 (C-3); 141.6 (C-7a); 127.4 (C-6); 120.2 (C-5); 119.1 (C-4); 112.8 (C-3a); 108.7 (C-7); 69.1 (O–CH_2); 54.9 (N1–CH_2); 54.3 (2C, CH_2); 47.6 (CH_2); 23.5 (2C, CH_2); 133.7 (C, Ar); 132.7 (C, Ar); 131.9 (C, Ar); 129.0 (C, Ar); 128.6 (C, Ar); 127.1 (C, Ar); 127.2 (C, Ar); 126.4 (C, Ar); 125.9 (C, Ar); 125.3 (C, Ar); 124.1 (C, Ar). HPLC-MS (ES^+): CH_3CN/H_2O 10:100, gt: 6 min; rt: 3.53, $[M + H]^+ = 372.3$.

4.1.13. 3-(1-Naphthylmethoxy)-1-(2-piperidinoethyl)indazole (**7**)

Following the procedure B, from **32** (0.30 g, 1.11 mmol), 2-piperidinoethyl chloride hydrochloride (0.23 g, 1.20 mmol) and K_2CO_3 (0.69 g, 5.00 mmol) in 2-butanone (60 mL). The final product was purified by chromatography column using as eluent dichloromethane:methanol (1:0, 30:1). Reaction time: 24 h. Yield: (0.25 g, 59%). Oil. ^1H NMR (300 MHz, $CDCl_3$) δ: 7.89 (d, 1H, 4-H); 7.62 (d, 1H, 7-H); 7.49 (t, 1H, 5-H); 7.00 (t, 1H, 6-H); 8.20–7.34 (m, 7H, Ar); 5.86 (s, 2H, O–CH_2); 4.40 (t, 2H, N1–CH_2); 2.89 (t, 2H, CH_2); 2.54 (m, 4H, CH_2); 1.62 (m, 4H, CH_2); 1.25 (m, 2H, CH_2). ^{13}C NMR (300 MHz, $CDCl_3$) δ: 155.8 (C-3); 141.6 (C-7a); 127.1 (C-6); 120.1 (C-5); 119.1 (C-4); 112.7 (C-3a); 108.8 (C-7); 69.1 (O–CH_2); 57.5 (N1–CH_2); 54.7 (2C, CH_2); 46.1 (CH_2); 25.8 (2C, CH_2); 24.1 (CH); 133.7 (C, Ar); 132.7 (C, Ar); 131.9 (C, Ar); 129.0 (C, Ar); 128.6 (C, Ar); 127.1 (C, Ar); 127.2 (C, Ar); 126.4 (C, Ar); 125.9 (C, Ar); 125.3 (C, Ar); 124.1 (C, Ar). HPLC-MS (ES^+): CH_3CN/H_2O 20:100, gt: 20 min; rt: 9.57, $[M + H]^+ = 386.0$.

4.1.14. 3-(1-Naphthylmethoxy)-1-(1-naphthylmethyl)indazole (**8**)

Following the procedure A, from **26** (0.050 g, 0.38 mmol), 1-naphthylmethyl chloride (0.150 g, 0.85 mmol) and Cs_2CO_3 (0.325 g, 1.00 mmol) in acetone (40 mL). Reaction time: 48 h. Yield: (0.09 g, 60%). Oil. ^1H NMR (300 MHz, DMSO-d_6) δ: 7.71 (dd, 1H, 4-H); 7.66 (d, 1H, 7-H); 7.37 (t, 1H, 5-H); 7.03 (t, 1H, 6-H); 8.27–7.15 (m, 14H, Ar); 5.94 (s, 2H, O–CH_2); 5.92 (s, 2H, N1–CH_2). ^{13}C NMR (300 MHz, DMSO-d_6) δ: 155.9 (C-3); 142.0 (C-7a); 127.3 (C-6); 120.3 (C-5); 119.2 (C-4); 113.2 (C-3a); 109.0 (C-7); 69.2 (O–CH_2); 50.9 (N1–CH_2); 133.8 (C, Ar); 132.8 (C, Ar); 132.6 (C, Ar); 131.9 (C, Ar); 131.1 (C, Ar); 129.0 (C, Ar); 128.9 (C, Ar); 128.6 (C, Ar); 127.4 (C, Ar); 126.4 (2C, Ar); 125.9 (2C, Ar); 125.4 (2C, Ar); 125.3 (2C, Ar); 125.2 (2C, Ar); 124.1 (2C, Ar); 123.2 (2C, Ar). HPLC-MS (ES^+): CH_3CN/H_2O 10:90, gt: 6 min; rt: 6.66, $[M + H]^+ = 415.5$.

4.1.15. 3-(2-Naphthylmethoxy)-1-(2-piperidinoethyl)indazole (**9**)

Following the procedure B, from **33** (0.30 g, 1.10 mmol), 2-piperidinoethyl chloride hydrochloride (0.20 g, 1.10 mmol) and K_2CO_3 (0.62 g, 4.49 mmol) in 2-butanone (60 mL). The final product was purified by chromatography column using as eluent dichloromethane:methanol (1:0, 30:1). Reaction time: 24 h. Yield: (0.27 g, 64%). Oil. ^1H NMR (300 MHz, $CDCl_3$) δ: 7.68 (dd, 1H, 4-H); 7.35 (t, 1H, 5-H); 7.27 (dd, 1H, 7-H); 7.02 (t, 1H, 6-H); 7.98–7.25 (m, 7H, Ar); 5.59 (s, 2H, O–CH_2); 4.35 (t, 2H, N1–CH_2); 2.79 (t, 2H, CH_2); 2.46 (m, 4H, CH_2); 1.55 (m, 4H, CH_2); 1.41 (m, 2H, CH_2). ^{13}C NMR (300 MHz, $CDCl_3$) δ: 155.6 (C-3); 141.6 (C-7a); 127.0 (C-6); 120.1 (C-5); 119.0 (C-4); 112.6 (C-3a); 108.7 (C-7); 70.7 (O–CH_2); 57.7 (N1–CH_2); 54.7 (2C, CH_2); 46.3 (CH_2); 25.8 (2C, CH_2); 24.1 (CH_2); 134.6 (C, Ar); 133.3 (C, Ar); 133.1 (C, Ar); 128.1 (C, Ar); 128.0 (C, Ar); 127.7 (C, Ar); 127.2 (C, Ar); 126.1 (C, Ar); 126.0 (C, Ar); 125.9 (C, Ar). HPLC-MS (ES^+): CH_3CN/H_2O 10:90, gt: 8 min; rt: 3.54, $[M + H]^+ = 386.3$.

4.1.16. 5–Nitro-1-(pentyl)-3-(pentyloxy)indazole (**10**)

Following the procedure A, from **27** (0.37 g, 2.07 mmol), pentyl iodide (0.57 mL, 4.35 mmol) and K_2CO_3 (0.70 g, 5.07 mmol) in acetone (60 mL). Reaction time: 120 h. Yield: (0.42 g, 65%). Oil. ^1H NMR (300 MHz, DMSO-d_6) δ: 8.47 (d, 1H, 4-H); 8.18 (dd, 1H, 6-H); 7.49 (d, 1H, 7-H); 4.35 (t, 2H, O–CH_2); 4.26 (t, 2H, N1–CH_2); 1.79–1.11 (m, 12H, 2(CH_2)$_3$); 0.86 (t, 3H, CH_3); 0.77 (t, 3H, CH_3). ^{13}C NMR

(300 MHz, DMSO-d_6) δ: 156.9 (C-3); 142.2 (C-7a); 140.1 (C-5); 122.0 (C-6); 117.5 (C-4); 110.7 (C-3a); 110.1 (C-7); 69.1 (O–CH_2); 48.1 (N1–CH_2); 28.8 (CH_2); 28.3 (CH_2); 28.2 (CH_2); 27.6 (CH_2); 21.9 (CH_2); 21.7 (CH_2); 13.9 (CH_3); 13.8 (CH_3). HPLC-MS (ES^+): CH_3CN/H_2O 20:80, gt: 6 min; rt: 4.51, $[M + H]^+ = 320.3$.

4.1.17. 1-Benzyl-3-cyclohexylmethoxy-5-nitroindazole (**11**)

Following the procedure C **28** (0.10 g, 0.38 mmol), cyclohexylmethyl bromide (0.10 mL, 0.70 mmol) and K_2CO_3 (0.14 g, 0.98 mmol) in 2-butanone (60 mL). The product was purified by silica gel column chromatography using as eluent a mixture dichloromethane:hexane (1:1, 5:1). Reaction time: 24 h. Yield: (0.078 g, 60%). Mp 72–75 °C (2-propanol). ^{1}H NMR (300 MHz, $CDCl_3$) δ: 8.67 (d, 1H, 4-H); 8.17 (dd, 1H, 6-H); 7.30 (d, 1H, 7-H); 7.29–7.15 (m, 5H, Ar); 5.41 (s, 2H, N1–CH_2); 4.20 (d, 2H, O–CH_2); 1.93–1.09 (m, 11H, Cy). ^{13}C NMR (300 MHz, $CDCl_3$) δ: 158.7 (C-3); 143.1 (C-5); 141.3 (C-7a); 137.6 (C, Ar); 129.3 (2C, Ar); 128.4 (C, Ar); 127.5 (2C, Ar); 123.0 (C-6); 119.2 (C-4); 113.2 (C-3a); 109.2 (C-7); 71.5 (O–CH_2); 53.3 (N1–CH_2); 38.0 (CH_2); 30.1 (2C, CH_2); 26.9 (CH_3); 26.2 (2C, CH_2). HPLC-MS (ES^+): CH_3CN/H_2O 10:90, gt: 8 min; rt: 7.07, $[M + H]^+ = 366.4$.

4.1.18. 3-(4-Methoxybenzyloxy)-5-nitro-1-pentylindazole (**13**)

Following the procedure B, from **34** (0.20 g, 0.67 mmol), 1-pentyl iodide (0.1 mL, 0.77 mmol) and K_2CO_3 (0.35 g, 2.50 mmol) in 2-butanone (60 mL). The final product was purified by chromatography column using as eluent dichloromethane:hexane (1:1, 5:1). Reaction time: 72 h. Yield: (0.07 g, 30%). Mp 78–80 °C. ^{1}H NMR (300 MHz, $CDCl_3$) δ: 8.66 (d, 1H, 4-H); 8.20 (dd, 1H, 6-H); 7.45 (2H, Ar); 7.23 (d, 1H, 7-H); 6.93 (2H, Ar); 5.36 (s, 2H, O–CH_2); 4.20 (t, 2H, N1–CH_2); 3.83 (s, 3H, O–CH_3); 1.89 (q, 2H, CH_2); 1.36–1.22 (m, 4H, 2CH_2); 0.88 (s, 3H, CH_3). ^{13}C NMR (300 MHz, $CDCl_3$) δ: 159.8 (C–OCH_3); 157.5 (C-3); 142.5 (C-7a); 140.7 (C-5); 130.1 (2C, Ar); 128.4 (Ar); 122.4 (C-6); 118.8 (C-4); 113.9 (2C, Ar); 112.0 (C-3a); 108.4 (C-7); 70.9 (O–CH_2); 55.31 (O–CH_3); 48.9 (N1–CH_2); 29.3 (CH_2); 28.9 (CH_2); 22.3 (CH_2); 13.9 (CH_3). HPLC-MS (ES^+): CH_3CN/H_2O 20:100, gt: 20 min; rt: 16.89, $[M + H]^+ = 370.3$.

4.1.19. 1-(2-Diisopropylaminoethyl)-3-(4-methoxybenzyloxy)-5-nitroindazole (**14**)

Following the procedure B, from **34** (0.100 g, 0.33 mmol), 2-diisopropylaminoethyl chloride hydrochloride (0.07 g, 0.33 mmol) and K_2CO_3 (0.12 g, 0.90 mmol) in 2-butanone (60 mL). The solvent was evaporated under reduced pressure. Then, the solid is suspended in water and extracted with diethylic ether. After evaporate the ether fraction, the solid obtained is recrystallized from 2-propanol. Reaction time: 6 h. Yield: (0.12 g, 82%). Mp 83–85 °C. ^{1}H NMR (300 MHz, $CDCl_3$) δ: 8.63 (d, 1H, 4-H); 8.18 (dd, 1H, 6-H); 7.47 (d, 2H, Ar); 7.27 (d, 1H, 7-H); 6.93 (d, 2H, Ar); 5.37 (s, 2H, O–CH_2); 4.17 (t, 2H, N1–CH_2); 3.83 (s, 3H, O–CH_3); 2.95 (m, 2H, CH); 2.85 (t, 2H, CH_2); 0.91 (d, 12H, CH_3). ^{13}C NMR (300 MHz, $CDCl_3$) δ: 160.2 (C–OCH_3); 158.0 (C-3); 142.5 (C-7a); 140.7 (C-5); 130.1 (2C, Ar); 129.4 (Ar); 122.6 (C-6); 119.1 (C-4); 114.4 (2C, Ar); 112.2 (C-3a); 109.5 (C-7); 71.3 (O–CH_2); 55.3 (O–CH_3); 50.2 (N1–CH_2); 49.3 (2C, CH); 45.2 (CH_2); 21.1 (4C, CH_3). HPLC-MS (ES^+): CH_3CN/H_2O 10:90, gt: 6 min; rt: 3.36, $[M + H]^+ = 427.3$.

4.1.20. 3-(1-Naphthylmethoxy)-5-nitro-1-(2-(pyrrolidin-1-yl) ethyl)indazole (**15**)

Following the procedure B, from **35** (0.20 g, 0.62 mmol), 2-pyrrolydinnoethyl chloride hydrochloride (0.17 g, 1.00 mmol) and K_2CO_3 (0.28 g, 2.00 mmol) in butanone (60 mL). The final product was purified by chromatography column using as eluent dichloromethane:methanol (1:0, 30:1). Reaction time: 60 h. Yield: (0.20 g, 76%). Oil. ^{1}H NMR (300 MHz, $CDCl_3$) δ: 8.64 (d, 1H, 4-H); 8.29 (dd, 1H, 6-H); 8.18 (dd, 1H, Ar); 7.51 (d, 1H, 7-H); 7.93–7.58 (m, 6H, Ar); 5.91 (s, 2H, O–CH_2); 4.84 (t, 2H, N1–CH_2); 3.49 (s, 2H, CH_2); 2.84 (m, 4H, CH_2); 1.91 (m, 4H, CH_2). ^{13}C NMR (300 MHz, $CDCl_3$) δ: 158.4 (C-3); 143.85 (C-7a); 142.1 (C-5); 123.9 (C-6); 118.8 (C-4); 112.2 (C-7); 110.2 (C3a); 69.9 (O–CH_2); 54.3 (2C, CH); 53.9 (N1–CH_2); 45.8 (CH_2); 23.7 (2C, CH_2); 133.7 (C, Ar); 132.7 (C, Ar); 131.9 (C, Ar); 129.0 (C, Ar); 128.6 (C, Ar); 127.1 (C, Ar); 127.2 (C, Ar); 126.4 (C, Ar); 125.9 (C, Ar); 125.3 (C, Ar); 124.1 (C, Ar). HPLC-MS (ES^+): CH_3CN/H_2O 15:95, gt: 6 min; rt: 3.28, $[M + H]^+ = 417.4$.

4.1.21. 3-(1-Naphthylmethoxy)-1-(1-naphthylmethyl)-5-nitroindazole (**16**)

Following the procedure A from **27** (0.35 g, 1.95 mmol), 1-naphthylmethyl chloride (0.83 g, 4.72 mmol) and Cs_2CO_3 (1.80 g, 5.52 mmol) in acetone (60 mL). Reaction time: 72 h. Yield: (0.717 g, 68%). Mp 143–145 °C* (decomp) (2-propanol). ^{1}H NMR (300 MHz, DMSO-d_6) δ: 8.75 (d, 1H, 4-H); 8.23 (dd, 1H, 6-H); 7.25 (d, 1H, 7-H); 8.30–7.37 (m, 14H, Ar); 6.06 (s, 2H, O–CH_2); 6.05 (s, 2H, N1–CH_2). ^{13}C NMR (300 MHz, DMSO-d_6) δ: 157.9 (C-3); 143.5 (C-5); 141.5 (C-7a); 122.6 (C-6); 118.7 (C-4); 112.7 (C-7); 109.0 (C-3a); 70.0 (O–CH_2); 52.1 (N1–CH_2); 133.8 (C, Ar); 133.7 (C, Ar); 131.7 (C, Ar); 131.6 (C, Ar); 131.4 (C, Ar); 131.0 (C, Ar); 129.4 (C, Ar); 129.0 (C, Ar); 128.9 (C, Ar); 128.7 (C, Ar); 127.6 (C, Ar); 126.7 (C, Ar); 126.6 (C, Ar); 126.1 (C, Ar); 126.0 (C, Ar); 125.6 (C, Ar); 125.3 (C, Ar); 125.2 (C, Ar); 123.7 (C, Ar); 123.0 (C, Ar). HPLC-MS (ES^+): CH_3CN/H_2O, 10:90 gt: 6 min; rt: 6.65, $[M + H]^+ = 460.2$.

4.1.22. 3-(2-Naphthylmethoxy)-5-nitro-1-pentylindazole (**17**)

Following the procedure B, from **36** (0.21 g, 0.67 mmol), 1-pentyl iodide (0.1 mL, 0.76 mmol) and K_2CO_3 (0.39 g, 2.82 mmol) in acetone (60 mL). The final product was purified by chromatography column using as eluent dichloromethane:hexane (1:1, 5:1). Reaction time: 120 h. Yield: (0.10 g, 58%). Mp 104–106 °C (2-propanol). ^{1}H NMR (300 MHz, $CDCl_3$) δ: 8.72 (d, 1H, 4-H); 8.24 (dd, 1H, 6-H); 7.52 (d, 1H, 7-H); 7.98–7.23 (m, 7H, Ar); 5.61 (s, 2H, O–CH_2); 4.21 (t, 2H, N1–CH_2); 1.90 (q, 2H, CH_2); 1.29 (m, 4H, 2CH_2); 0.87 (t, 3H, CH_3). ^{13}C NMR (300 MHz, $CDCl_3$) δ: 157.4 (C-3); 142.5 (C-7a); 140.8 (C-5); 122.4 (C-6); 118.8 (C-4); 111.9 (C-3a); 108.5 (C-7); 71.16 (O–CH_2); 49.0 (N1–CH_2); 29.3 (CH_2); 28.9 (CH_2); 22.5 (CH_2); 13.9 (CH_3), 133.7 (C, Ar); 133.2 (C, Ar); 128.3 (C, Ar); 128.0 (C, Ar); 127.7 (C, Ar); 127.2 (C, Ar); 126.3 (C, Ar); 126.2 (C, Ar); 125.8 (C, Ar). HPLC-MS (ES^+): CH_3CN/H_2O 15:95, gt: 8 min; rt: 7.44, $[M + H]^+ = 390.4$.

4.1.23. 3-(2-Naphthylmethoxy)–5–nitro-1-(2-piperidinoethyl) indazole (**18**)

Following the procedure B, from **36** (0.21 g, 0.67 mmol), 2-piperidinoethyl chloride hydrochloride (0.12 g, 0.67 mmol) and K_2CO_3 (0.65 g, 4.71 mmol) in 2-butanone (60 mL). The solvent was evaporated under reduced pressure. Then, the solid is suspended in water and extracted with chloroform. After evaporate the organic phase, the solid obtained is recrystallized from 2-propanol. Reaction time: 72 h. Yield: (0.17 g, 60%). Mp 83–86 °C (2-propanol). ^{1}H NMR (300 MHz, $CDCl_3$) δ: 8.70 (d, 1H, 4-H); 8.22 (dd, 1H, 6-H); 7.28 (d, 1H, 7-H); 7.98–7.49 (m, 7H, Ar); 5.60 (s, 2H, O–CH_2); 4.32 (t, 2H, N1–CH_2); 2.77 (t, 2H, CH_2); 2.39 (d, 4H, CH_2); 1.48 (d, 4H, CH_2); 1.39 (d, 2H, CH_2). ^{13}C NMR (300 MHz, $CDCl_3$) δ: 157.5 (C-3); 143.1 (C-7a); 140.8 (C-5); 122.3 (C-6); 118.6 (C-4); 112.0 (C-3a); 109.0 (C-7); 71.2 (O–CH_2); 57.8 (N1–CH_2); 54.7 (2C, CH_2); 46.3 (CH_2); 25.8 (2C, CH_2); 24.1 (CH_2); 133.7 (C, Ar); 133.2 (C, Ar); 128.3 (C, Ar); 128.0 (C, Ar); 127.7 (C, Ar); 127.2 (C, Ar); 126.3 (C, Ar); 126.2 (C, Ar); 125.8 (C, Ar). HPLC-MS (ES^+): CH_3CN/H_2O 5:95, gt: 20 min; rt: 12.54, $[M + H]^+ = 431.2$.

*4.1.24. 1-(2-Morpholinoethyl)-3-(2-naphthylmethoxy)-5-nitroindazole (**19**)*

Following the procedure B, from **36** (0.09 g, 0.28 mmol), 2-morpholinoethyl chloride hydrochloride (0.07 g, 0.40 mmol) and K_2CO_3 (0.15 g, 0.81 mmol) in 2-butanone (60 mL). The solvent was evaporated under reduced pressure. Then, the solid is suspended in water and extracted with chloroform. After evaporate the organic phase, the solid obtained is recrystallized from 2-propanol. Reaction time: 98 h. Yield: (0.11 g, 94%). Mp 104–106 °C (2-propanol). ^{1}H NMR (300 MHz, $CDCl_3$) δ: 8.71 (d, 1H, 4-H); 8.23 (dd, 1H, 6-H); 7.51 (d, 1H, 7-H); 7.98–7.49 (m, 7H, Ar); 5.60 (s, 2H, O–CH_2); 4.34 (t, 2H, N1–CH_2); 3.58 (d, 4H, CH_2); 2.83 (t, 2H, CH_2); 2.43 (d, 4H, CH_2). ^{13}C NMR (300 MHz, $CDCl_3$) δ: 157.5 (C-3); 143.1 (C-7a); 140.9 (C-5); 122.3 (C-6); 118.7 (C-4); 112.1 (C-3a); 108.8 (C-7); 71.2 (2C, CH_2); 66.8 (O–CH_2); 57.3 (N1–CH_2); 53.7 (2C, CH_2); 46.7 (CH_2); 133.6 (C, Ar); 133.1 (C, Ar); 128.4 (C, Ar); 128.0 (C, Ar); 127.7 (C, Ar); 127.2 (C, Ar); 126.4 (C, Ar); 126.3 (C, Ar); 125.7 (C, Ar). HPLC-MS (ES^+): CH_3CN/H_2O 20:100, gt: 20 min; rt: 11.60, $[M + H]^+ = 433.45$.

*4.1.25. 1-Benzyl-3-(2-naphthylmethoxy)-5-nitroindazole (**20**)*

Following the procedure C, from **28** (0.29 g, 1.07 mmol), 2-naphthylmethyl bromide (0.25 g, 1.12 mmol) and Cs_2CO_3 (1.20 g, 3.7 mmol) in acetone (60 mL). the product was purified by recrystallization from 2-propanol. Reaction time: 72 h. Yield: (0.201 g, 45%). Mp 100–103 °C (2-propanol). ^{1}H NMR (300 MHz, DMSO-d_6) δ: 8.60 (d, 1H, 4-H); 8.22 (dd, 1H, 6-H); 7.83 (d, 1H, 7-H); 8.09–7.21 (m, 12H, Ar); 5.62 (s, 2H, O–CH_2); 5.56 (s, 2H, N1–CH_2). ^{13}C NMR (300 MHz, DMSO-d_6) δ: 156.8 (C-3); 142.6 (C-7a); 140.6 (C-5); 122.4 (C-6); 117.7 (C-4); 112.8 (C-3a); 108.6 (C-7); 70.7 (O–CH_2); 51.8 (N1–CH_2); 136.8 (C, Ar); 133.8 (C, Ar); 132.7 (C, Ar); 132.6 (C, Ar); 128.5 (2C, Ar); 128.0 (C, Ar); 127.9 (C, Ar); 127.6 (C, Ar); 127.5 (C, Ar); 127.3 (2C, Ar); 127.0 (C, Ar); 126.3 (C, Ar); 126.0 (C, Ar). HPLC-MS (ES^+): CH_3CN/H_2O 10:90, gt: 6 min; rt: 6.40, $[M + H]^+ = 410.3$.

*4.1.26. 3-(2-Naphthylmethoxy)-1-(2-naphthylmethyl)-5-nitroindazole (**21**)*

Following the procedure A, from **27** (0.31 g, 1.73 mmol), 2-naphthylmethyl bromide (1.21 mL, 5.48 mmol) and K_2CO_3 (0.73 g, 5.28 mmol) in acetone (60 mL). Reaction time: 72 h. Yield: (0.31 g, 30%). Mp 101–103 °C (2-propanol). ^{1}H NMR (300 MHz, DMSO-d_6) δ: 8.73 (d, 1H, 4-H); 8.18 (dd, 1H, 6-H); 7.48 (d, 1H, 7-H); 7.98–7.23 (m, 14H, Ar); 5.64 (s, 2H, O–CH_2); 5.59 (s, 2H, N1–CH_2). ^{13}C NMR (300 MHz, DMSO-d_6) δ: 157.6 (C-3); 142.8 (C-7a); 141.1 (C-5); 122.7 (C-6); 118.7 (C-4); 112.7 (C-7); 108.9 (C-3a); 71.3 (O–CH_2); 53.2 (N1–CH_2); 133.6 (C, Ar); 133.5 (C, Ar); 133.2 (C, Ar); 132.9 (C, Ar); 128.8 (C, Ar); 128.4 (C, Ar); 128.0 (C, Ar); 127.8 (C, Ar); 127.7 (C, Ar); 127.3 (C, Ar); 126.5 (C, Ar); 126.3 (C, Ar); 126.1 (C, Ar); 125.8 (C, Ar); 124.8 (C, Ar). HPLC-MS (ES^+): CH_3CN/H_2O 70:100, gt: 15 min; rt: 9.65, $[M + H]^+ = 460.2$.

*4.1.27. 5-Amino-1-benzyl-3-benzyloxyindazole (**22**)*

Following the procedure D, from **12** (0.22 g, 0.60 mmol), hydrazine monohydrated (0.60 mL, 1.6 mmol) and FeO(OH) (0.05 g, 0.5 mmol) in methanol (30 mL). The product was purified by extraction water/chloroform and evaporation of this one. Reaction time: 24 h. Yield: (0.191 g, 97%). Oil. ^{1}H NMR (300 MHz, DMSO-d_6) δ: 7.48–7.11 (m, 10H, Ar); 7.24 (d, 1H, 7-H); 6.65 (d, 1H, 4-H); 6.77 (dd, 1H, 6-H); 5.32 (s, 2H, O–CH_2); 5.30 (s, 2H, N1–CH_2); 4.80 (br s, 2H, NH_2). ^{13}C NMR (300 MHz, DMSO-d_6) δ: 153.7 (C-3); 141.9 (C-5); 136.3 (C-7a); 119.1 (C-6); 112.9 (C-3a); 110.1 (C-7); 99.6 (C-4); 69.8 (O–CH_2); 51.4 (N1–CH_2); 138.2 (C, Ar); 137.2 (C, Ar); 128.3 (2C, Ar); 127.9 (2C, Ar); 127.8 (C, Ar); 127.1 (2C, Ar). HPLC-MS (ES^+): CH_3CN/H_2O 10:100, gt: 6 min; rt: 3.71, $[M + H]^+ = 330.2$.

*4.1.28. 5-Amino-3-(1-naphthylmethoxy)-1-(2-(pyrrolidin-1-yl)ethyl)indazole (**23**)*

Following the procedure D, from **15** (0.08 g, 0.20 mmol), hydrazine monohydrated (3.50 mL, 9.23 mmol) and FeO(OH) (0.04 g, 0.4 mmol) in methanol (30 mL). The product was purified by chromatography column using as eluent the mixture dichloromethane:methanol (1:0, 20:1). Reaction time: 30 h. Yield: (0.06 g, 85%). Mp 136–138 °C. ^{1}H NMR (300 MHz, $CDCl_3$) δ: 8.19–7.45 (m, 7H, Ar); 7.16 (d, 1H, 7-H); 6.84 (m, 2H, 4-H, 6-H); 5.83 (s, 2H, O–CH_2); 4.37 (t, 2H, N1–CH_2); 3.57 (br s, 2H, NH_2); 3.01 (t, 2H, CH_2); 2.61 (s, 4H, CH_2); 1.78 (d, 4H, CH_2). ^{13}C NMR (300 MHz, $CDCl_3$) δ: 155.3 (C-3); 139.6 (C-5); 137.9 (C-7a); 119.9 (C-6); 113.7 (C-3a); 110.0 (C-7); 103.4 (C-4); 69.5 (O–CH_2); 55.3 (N1–CH_2); 54.7 (2C, CH_2); 48.0 (CH_2); 23.9 (2C, CH_2); 133.7 (C, Ar); 132.7 (C, Ar); 131.9 (C, Ar); 129.0 (C, Ar); 128.6 (C, Ar); 127.1 (C, Ar); 127.2 (C, Ar); 126.4 (C, Ar); 125.9 (C, Ar); 125.3 (C, Ar); 124.1 (C, Ar). HPLC-MS (ES^+): CH_3CN/H_2O 15:95, gt: 6 min; rt: 2.05, $[M + H]^+ = 387.4$.

*4.1.29. 5-Amino-3-(2-naphthylmethoxy)-1-(2-piperidinoethyl)indazole (**24**)*

Following the procedure D, from **18** (0.11 g, 0.25 mmol), hydrazine monohydrated (1.20 mL, 3.16 mmol) and FeO(OH) (0.02 g, 0.2 mmol) in methanol (30 mL). The product was purified by chromatography column using as eluent the mixture dichloromethane:methanol (1:0, 20:1). Reaction time: 24 h. Yield: (0.07 g, 66%). Oil. ^{1}H NMR (300 MHz, $CDCl_3$) δ: 7.96–7.47 (m, 7H, Ar); 7.11 (d, 1H, 7-H); 6.91 (s, 1H, 4-H); 6.83 (d, 1H, 6-H); 5.54 (s, 2H, O–CH_2); 4.27 (t, 2H, N1–CH_2); 3.26 (br s, 2H, NH_2); 2.73 (t, 2H, CH_2); 2.42 (d, 4H, CH_2); 1.56 (d, 4H, CH_2); 1.41 (d, 2H, CH_2). ^{13}C NMR (300 MHz, $CDCl_3$) δ: 154.9 (C-3); 139.2 (C-5); 137.7 (C-7a); 119.5 (C-6); 113.3 (C-3a); 109.9 (C-7); 103.2 (C-4); 71.0 (O–CH_2); 58.1 (N1–CH_2); 55.0 (2C, CH_2); 46.7 (CH_2); 26.1 (2C, CH_2); 24.4 (CH_2); 133.6 (C, Ar); 133.1 (C, Ar); 128.4 (C, Ar); 128.0 (C, Ar); 127.7 (C, Ar); 127.2 (C, Ar); 126.4 (C, Ar); 126.3 (C, Ar); 125.7 (C, Ar). HPLC-MS (ES^+): CH_3CN/H_2O 10:100, gt: 6 min; rt: 2.33, $[M + H]^+ = 401.2$.

*4.1.30. 5-Bromo-3-(2-naphthylmethoxy)-1-(2-piperidinoethyl)indazole (**25**)*

From **9** (0.09 g, 0.24 mmol) in acetonitrile (20 mL), iron trichloride hexahydrate (0.05 g, 0.17 mmol) was added. The reaction mixture was heated to 80 °C and then, N-bromosuccinimide (0.04 g, 0.20 mmol) was added. The reaction was heated for 40 h. The solvent is evaporated under reduced pressure and the residue is extracted with water/chloroform. After evaporation of the chloroform, The product was purified by chromatography column using as eluent the mixture dichloromethane:methanol (1:0, 10:1). Reaction time: 40 min. Yield: (0.03 g, 27%). Oil. ^{1}H NMR (300 MHz, $CDCl_3$) δ: 7.83 (d, 1H, 4-H); 7.41 (dd, 1H, 6-H); 7.20 (dd, 1H, 5-H); 7.96–7.47 (m, 7H, Ar); 5.56 (s, 2H, O–CH_2); 4.35 (t, 2H, N1–CH_2); 2.81 (t, 2H, CH_2); 2.43 (d, 4H, CH_2); 1.55 (d, 4H, CH_2); 1.39 (d, 2H, CH_2). ^{13}C NMR (300 MHz, $CDCl_3$) δ: 154.8 (C-3); 140.3 (C-7a); 130.3 (C-6); 122.6 (C-4); 114.1 (C-5); 111.8 (C-3a); 110.4 (C-7); 70.8 (O–CH_2); 57.5 (N1–CH_2); 54.7 (2C, CH_2); 46.4 (CH_2); 25.5 (2C, CH_2); 23.9 (CH_2); 134.3 (C, Ar); 133.2 (C, Ar); 133.1 (C, Ar); 128.2 (C, Ar); 128.0 (C, Ar); 127.7 (C, Ar); 127.0 (C, Ar); 126.2 (C, Ar); 126.1 (C, Ar); 125.8 (C, Ar). HPLC-MS (ES^+): CH_3CN/H_2O 5:80, gt: 20 min; rt: 15.28, $[M + H]^+ = 467.1$.

*4.1.31. 3-(4-Methoxybenzyloxy)-1H-indazole (**31**) and 2-(4-methoxybenziloxy)-1H-3-indazolone (**37**)*

Following the procedure E, from **29** (1.50 g, 7.27 mmol), 4-methoxybenzyl bromide (1.3 mL, 9.0 mmol) and K_2CO_3 (2.20 g, 16.16 mmol) in 1,4-dioxane (100 mL). Reaction time: 24 h. Total yield: (1.42 g, 77%). Yield **31**: 0.61 g (33%). Mp 73–76 °C. ^{1}H NMR (300 MHz, $CDCl_3$) δ: 8.86 (s, 1H, NH); 7.70 (d, 1H, 4-H); 7.46 (d, 2H, Ar); 7.37 (t, 1H, 5-H); 7.30 (d, 1H, 7-H); 7.08 (t, 1H, 6-H); 6.93 (d, 2H,

Ar); 5.38 (s, 2H, O–CH_2); 3.83 (s, 3H, O–CH_3). ^{13}C NMR (300 MHz, $CDCl_3$) δ: 159.6 (C, Ar), 157.6 (C-3); 142.6 (C-7a); 129.8 (2C, Ar); 129.1 (C, Ar); 127.8 (C-6); 120.0 (C-5); 119.8 (C-4); 113.9 (2C, Ar); 112.9 (C-3a); 109.6 (C-7); 70.4 (O–CH_2); 55.3 (O–CH_3) HPLC-MS (ES^+): CH_3CN/H_2O 5:95, gt: 20 min, rt: 13.31, $[M + H]^+ = 179.7$. Yield **37**: 0.81 g (44%). Mp 165–167 °C. ^{1}H NMR (300 MHz, DMSO) δ: 10.26 (br s, 1H, NH); 7.67 (d, 1H, 4-H); 7.49 (t, 1H, 5-H); 7.21 (d, 3H, 7-H, Ar); 7.09 (t, 1H, 6-H); 6.90 (d, 2H, Ar); 4.91 (s, 2H, N2–CH_2); 3.72 (s, 3H, O–CH_3). ^{13}C NMR (300 MHz, DMSO) δ: 160.5 (C, Ar), 158.6 (C-3); 145.9 (C-7a); 131.3 (C, Ar); 129.1 (2C, Ar); 128.8 (C-6); 122.9 (C-5); 120.7 (C-4); 117.0 (C-3a); 113.8 (2C, Ar); 112.1 (C-7); 55.0 (N2–CH_2); 46.2 (O–CH_3). HPLC-MS (ES^+): CH_3CN/H_2O 10:90, gt: 6 min, rt: 3.70, $[M + H]^+ = 255.0$.

4.1.32. 3-(1-Naphthylmethoxy)-1H-indazole (**32**) and 2-(1-naphthylmethoxy)-1H-3-indazolone (**38**)

Following the procedure E, from **29** (0.89 g, 4.33 mmol), 1-naphthylmethyl chloride (0.76 g, 4.33 mmol) and K_2CO_3 (1.63 g, 11.7 mmol) in butanone (80 mL). Reaction time: 48 h (0.65 g, 54%). Total yield: (0.72 g, 54%). Yield **32**: (0.59 g, 49%). Mp 100–103 °C. ^{1}H NMR (300 MHz, DMSO-d_6) δ: 12.00 (s, 1H, NH); 7.72 (d, 1H, 4-H); 7.52 (d, 1H, 7-H); 7.35 (t, 1H, 5-H); 6.98 (t, 1H, 6-H); 8.15–7.30 (m, 7H, Ar); 5.85 (s, 2H, O–CH_2). ^{13}C NMR (300 MHz, DMSO-d_6) δ: 155.6 (C-3); 141.8 (C-7a); 127.1 (C-6); 119.0 (2C, C-4, C-5); 111.1 (C-7); 110.1 (C-3a); 68.3 (O–CH_2); 133.3 (C, Ar); 132.5 (C, Ar); 131.3 (C, Ar); 128.8 (C, Ar); 128.5 (C, Ar); 127.0 (C, Ar); 126.5 (C, Ar); 126.0 (C, Ar); 125.4 (C, Ar); 123.7 (C, Ar). HPLC-MS (ES^+): CH_3CN/H_2O 10:90, gt: 6 min; rt: 5.43, $[M + H]^+ = 275.2$. Yield **38**: 0.06 g (5%). Mp 195–199 °C. ^{1}H NMR (300 MHz, DMSO) δ: 8.35 (d, 1H, 4-H); 7.32 (t, 1H, 5-H); 7.08 (d, 1H, 7-H); 6.91 (t, 1H, 6-H); 7.96–7.41 (m, 7H, Ar); 5.44 (s, 2H, N2–CH_2). ^{13}C NMR (300 MHz, DMSO-d_6) δ: 159.6 (C-3); 146.2 (C-7a); 126.3 (C-6); 122.9 (C-5); 118.7 (C-4); 115.3 (C-3a); 112.4 (C-7); 44.9 (N2–CH_2); 133.2 (C, Ar); 132.8 (C, Ar); 130.8 (C, Ar); 130.0 (C, Ar); 128.4 (C, Ar); 128.1 (C, Ar); 127.0 (C, Ar); 125.8 (C, Ar); 125.3 (C, Ar); 123.7 (C, Ar). HPLC-MS (ES^+): CH_3CN/H_2O 10:90, gt: 6 min; rt: 4.24, $[M + H]^+ = 275.0$.

4.1.33. 3-(2-Naphthylmethoxy)-1H-indazole (**33**) and 2-(2-naphthylmethoxy)-1H-3-indazolone (**39**)

Following the procedure E, from **29** (0.84 g, 4.07 mmol), 2-naphthylmethyl bromide (0.95 g, 4.33 mmol) and K_2CO_3 (0.82 g, 5.92 mmol) in butanone (100 mL). Reaction time: 4 h (0.55 g, 49%). Total yield: (0.72 g, 49%). Yield **33**: (0.38 g, 34%). Mp 114–118 °C. ^{1}H NMR (300 MHz, DMSO-d_6) δ: 11.98 (s, 1H, NH); 7.65 (dd, 1H, 4-H); 7.34 (m, 2H, 5-H, 7-H); 7.02 (t, 1H, 6-H); 8.04–7.50 (7H, Ar); 5.56 (s, 2H, O–CH_2). ^{13}C NMR (300 MHz, $CDCl_3$) δ: 155.5 (C-3); 141.7 (C-7a); 126.6 (C-6); 119.1 (C-5); 119.0 (C-4); 111.1 (C-3a); 110.0 (C-7); 69.9 (O–CH_2); 134.7 (C, Ar); 132.7 (C, Ar); 132.5 (C, Ar); 127.9 (C, Ar); 127.7 (C, Ar); 127.5 (C, Ar); 127.0 (C, Ar); 126.2 (C, Ar); 126.0 (C, Ar); 125.9 (C, Ar). HPLC-MS (ES^+): CH_3CN/H_2O 10:90, gt: 6 min; rt: 5.51, $[M + H]^+ = 275.3$. Yield **39**: 0.17 g (15%). Mp 206–210 °C, 205–212 °C. ^{1}H NMR (300 MHz, DMSO-d_6) δ: 10.29 (s, 1H, N1–H); 7.71 (d, 1H, 4-H); 7.49 (t, 1H, 5-H); 7.21 (d, 1H, 7-H); 7.12 (t, 1H, 6-H); 7.91–7.41 (m, 7H, Ar); 5.16 (s, 2H, N2–CH_2). ^{13}C NMR (300 MHz, DMSO-d_6) δ: 161.2 (C-3); 146.6 (C-7a); 126.7 (C-6); 123.5 (C-5); 121.3 (C-4); 117.5 (C-3a); 112.6 (C-7); 47.4 (N2–CH_2); 134.8 (C, Ar); 133.2 (C, Ar); 132.8 (C, Ar); 131.9 (C, Ar); 128.7 (C, Ar); 127.0 (C, Ar); 127.9 (C, Ar); 126.5 (C, Ar); 126.2 (C, Ar). HPLC-MS (ES^+): CH_3CN/H_2O 10:90, gt: 6 min; rt: 4.30, $[M + H]^+ = 275.3$.

4.1.34. 3-(4-Methoxybenzyloxy)-5-nitro-1H-indazole (**34**) and 2-(4-methoxybenzyloxy)-5-nitro-3-indazolone (**40**)

Following the procedure E, from **30** (0.35 g, 1.38 mmol), 4-methoxybenzyl bromide (0.35 mL, 2.50 mmol) and K_2CO_3 (0.26 g, 1.85 mmol) in butanone (30 mL). Reaction time: 24 h. Total yield: (0.72 g, 63%). Yield **34**: (0.12 g, 30%). Mp 129–132 °C. ^{1}H NMR (300 MHz, DMSO-d_6) δ: 12.72 (s, 1H, NH); 8.49 (d, 1H, 4-H); 8.15 (dd, 1H, 6-H); 7.53 (d, 1H, 7-H); 7.47 (d, 2H, Ar); 6.95 (d, 2H, Ar); 5.35 (s, 2H, O–CH_2); 3.75 (s, 3H, O–CH_3). ^{13}C NMR: (300 MHz, DMSO-d_6) δ: 159.3 (Ar); 157.6 (C-3); 143.1 (C-7a); 140.3 (C-5); 130.0 (2C, Ar); 128.4 (C, Ar); 122.0 (C-6); 117.4 (C-4); 113.8 (2C, C, Ar); 110.9 (C-7); 110.6 (C-3a); 70.3 (O–CH_2); 55.1 (O–CH_3). HPLC-MS (ES^+): CH_3CN/H_2O 10:100, gt: 6 min, rt: 5.32, $[M + H]^+ = 300.2$. Yield **40**: 0.12 g (50%). 138–140 °C. ^{1}H NMR (300 MHz, DMSO) δ: 8.51 (s, 1H, 4-H); 8.26 (d, 1H, 6-H), 7.35 (d, 1H, 7-H); 7.23 (d, 2H, Ar); 6.91 (d, 2H, Ar); 5.00 (s, 2H, N2–CH_2); 3.72 (s, 3H, O–CH_3). ^{13}C NMR (300 MHz, DMSO) δ: 158.8 (C, Ar); 158.4 (C-3); 145.6 (C-7a); 140.3 (C-5); 129.1 (2C, Ar); 128.0 (C, Ar); 126.0 (C-6); 120.5 (C-4); 114.0 (2C, C, Ar); 111.9 (C-7); 111.6 (C-3a); 55.0 (N2–CH_2); 46.4 (O–CH_3). HPLC-MS (ES^+): CH_3CN/H_2O 10:90, gt: 6 min; rt: 3.91, $[M + H]^+ = 300.2$.

4.1.35. 3-(1-Naphthylmethoxy)-5-nitro-1H-indazole (**35**) and 2-(1-naphthylmethyl)-5-nitro-3-indazolone (**41**)

Following the procedure E, from **30** (0.90 g, 3.58 mmol), 1-naphthylmethyl chloride (0.91 g, 5.17 mmol) and K_2CO_3 (0.72 g, 5.23 mmol) in DMF (60 mL). Reaction time: 24 h. Total yield: (0.72 g, 63%). Yield **35**: (0.59 g, 52%). Mp 204–206 °C. ^{1}H NMR (300 MHz, DMSO-d_6) δ: 8.48 (d, 1H, 4-H); 7.77 (d, 1H, 7-H); 7.62 (dd, 1H, 6-H); 8.17–7.51 (m, 7H, Ar); 5.92 (s, 2H, O–CH_2). ^{13}C NMR (300 MHz, DMSO-d_6) δ: 157.6 (C-3); 143.4 (C-5); 140.2 (C-7a); 121.8 (C-6); 117.4 (C-4); 111.2 (C-7); 110.4 (C-3a); 68.9 (O–CH_2); 133.3 (C, Ar); 132.0 (C, Ar); 131.2 (C, Ar); 129.0 (C, Ar); 128.5 (C, Ar); 127.3 (C, Ar); 126.7 (C, Ar); 126.0 (C, Ar); 125.4 (C, Ar); 123.7 (C, Ar). HPLC-MS (ES^+): CH_3CN/H_2O 10:90, gt: 6 min; rt: 5.74 $[M + H]^+ = 320.4$. Yield **41**: (0.12 g, 11%) mp 212–213 °C (decomp.). ^{1}H NMR (300 MHz, DMSO) δ: 11.9 (br s, 1H, NH); 8.55 (s, 1H, 4-H); 8.26 (d, 1H, 6-H); 7.99–7.43 (m, 7H, Ar); 7.33 (d, 1H, 7-H); 5.54 (s, 2H, N2–CH_2). ^{13}C NMR (300 MHz, DMSO) δ: 155.2 (C-3); 146.5 (C-5); 141.0 (C-7a); 126.5 (C-6); 121.0 (C-4); 112.5 (C-7); 112.3 (C-3a); 45.5 (N2–CH_2); 133.8 (C, Ar); 131.7 (C, Ar); 131.1 (C, Ar); 129.2 (C, Ar); 129.0 (C, Ar); 127.7 (C, Ar); 127.1 (C, Ar); 125.8 (C, Ar); 123.7 (C, Ar). HPLC-MS (ES^+): CH_3CN/H_2O 15:95, gt: 6 min; rt: 4.53 $[M + H]^+ = 320.4$.

4.1.36. 3-(2-Naphthylmethoxy)-5-nitro-1H-indazole (**36**) and 2-naphthylmetyl-5-nitro-3-indazolone (**42**)

Following the procedure E, from **30** (0.96 g, 3.82 mmol), 2-naphthylmethyl bromide (0.87 g, 3.94 mmol) and K_2CO_3 (0.63 g, 4.52 mmol) in butanone (100 mL). Reaction time: 30 h. Total yield: (0.90 g, 74%). Yield **36**: 0.54 g, (45%) mp 161–163 °C. ^{1}H NMR (300 MHz, $CDCl_3$) δ: 9.27 (s, 1H, N1–H); 8.75 (d, 1H, 4-H); 8.27 (dd, 1H, 6-H); 7.50 (d, 1H, 7-H); 7.98–7.33 (7H, Ar); 5.63 (s, 2H, O–CH_2). ^{13}C NMR (300 MHz, $CDCl_3$) δ: 158.8 (C-3); 143.7 (C-5); 141.7 (C-7a); 123.1 (C-6); 118.4 (C-4); 112.3 (C-3a); 109.8 (C-7); 71.2 (O–CH_2); 133.5 (C, Ar); 133.2 (C, Ar); 128.4 (C, Ar); 128.0 (C, Ar); 127.8 (C, Ar); 127.1 (C, Ar); 126.3 (C, Ar); 125.6 (C, Ar). HPLC-MS (ES^+): CH_3CN/H_2O 10:90, gt: 8 min, rt: 5.53, $[M + H]^+ = 320.1$. Yield **42**: 0.36 g (29%). Mp 230–232 °C (decomp.). ^{1}H NMR (300 MHz, DMSO) δ: 12.88 (s, 1H, N1–H); 8.55 (s, 1H, 4-H); 8.26 (d, 1H, 6-H); 7.44 (d, 1H, 7-H); 7.92–7.34 (7H, Ar); 5.28 (s, 2H, N2–CH_2). ^{13}C NMR (300 MHz, DMSO) δ: 157.9 (C-3); 146.3 (C-5); 140.8 (C-7a); 126.1 (C-6); 121.1 (C-4); 117.9 (C-3a); 112.4 (C-7); 47.5 (N2–CH_2); 134.1 (C, Ar); 133.1 (C, Ar); 132.8 (C, Ar); 128.8 (C, Ar); 128.0 (C, Ar); 127.9 (C, Ar); 126.9 (C, Ar); 126.8 (C, Ar); 126.6 (C, Ar). HPLC-MS (ES^+): CH_3CN/H_2O 10:90, gt: 8 min, rt: 4.42, $[M + H]^+ = 320.2$.

4.2. Biological assays

4.2.1. Radioligand binding assays for CB1 and CB2 receptors

CB1/CB2 receptor binding studies were performed using membrane fractions of human $CB1/CB_2$ receptor transfected cells

purchased from Perkin–Elmer Life and Analytical Sciences (Boston, MA). HEK293EBNA membranes were resuspended in Tris buffer (50 mM Tris–HCl, 2.5 mM EDTA, 5 mM $MgCl_2$, 0.5 mg/mL BSA fatty acid free, pH 7.4). Fractions of the final membrane suspension (about 0.415 mg/mL of protein for CB1 and about 0.18 mg/mL of protein for CB2) were incubated at 30 °C for 90 min with 0.54 nM [^{3}H]-CP55940 (139.6 Ci/mmol) for CB1 and 0.33 nM [^{3}H]-CP55940 (139.6 Ci/mmol) for CB2, in the presence or absence of several concentrations of the competing drug, in a final volume of 0.2 mL for CB1 and 0.6 mL for CB2 of assay buffer (50 mM Tris–HCl, 2.5 mM EDTA, 5 mM $MgCl_2$, 0.5 mg/mL BSA fatty acid free, pH 7.4). Nonspecific binding was determined in the presence of 10 μM WIN 55,212-2. Silanized tubes were used throughout the experiment to minimize receptor binding loss due to tube adsorption. The reaction was terminated by rapid vacuum filtration with a filter mate Harvester apparatus (Perkin–Elmer) through Filtermat A GF/C filters presoaked in 0.05% polyethylenimine (PEI).

The filters were washed nine times with ice-cold buffer for CB1 (50 mM Tris–HCl, 2.5 mM EDTA, 5 mM $MgCl_2$, 0.5 mg/mL BSA fatty acid free, pH 7.4) for CB1 and CB2 (50 mM Tris–HCl, 2.5 mM EGTA, 5 mM $MgCl_2$, 1 mg/mL BSA fatty acid free, pH 7.5), and bound radioactivity was measured with a 1450 LSC & Luminescence counter Wallac MicroBeta TriLux (Perkin–Elmer). The binding assay showed the appropriate sensitivity to CB1 and CB2 ligands. Thus, WIN 55,212-2 inhibited the binding with a K_i value of 36.2 nM (CB1R) and WIN 55,212-2 and HU-308 inhibited the binding with K_i values of 3.7 and 11.2 nM (CB2R), respectively. For all binding experiments, competition binding curves were analyzed by using an iterative curve-fitting procedure GraphPad [51], which provided IC_{50} values for test compounds. K_i values were determined by the method of Cheng and Prusoff [66,67].

4.2.2. In vitro cholinesterase inhibition assays

AChE from human erythrocytes (min. 500 units/mg protein in buffered aqueous solution), BuChE from equine serum (10 units/mg protein, lyophilized powder), and BuChE from human serum (3 units/mg protein, lyophilized powder) were purchased from Sigma. Compounds were evaluated in 100 mM phosphate buffer pH 8.0 at 30 °C, using acetylthiocholine and butyrylthiocholine (0.4 mM) as substrates, respectively. In both cases, 5,5-dithio-bis(2-nitrobenzoic)acid (DTNB, Ellmans reagent, 0.2 mM) was used and the values of IC_{50} were calculated by UV spectroscopy from the absorbance changes at 412 nm. Experiments were performed in triplicate.

4.2.3. Kinetic study of BuChE/AChE inhibition

To investigate the mechanism of action of the compounds on AChE or BuChE, a kinetic analysis was performed. The experiments were carried out using combinations of four substrate concentrations, and three inhibitor concentrations. Double-reciprocal Lineweaver–Burk plotting of the data obtained, in which each point is mean of three different experiments, were analyzed.

Competitive inhibitors have the same *y*-intercept as uninhibited enzyme (since V_{max} is unaffected by competitive inhibitors the inverse of V_{max} also doesn't change) but there are different slopes and *x*-intercepts. Non-competitive inhibition produces plots with the same *x*-intercept as uninhibited enzyme (K_m is unaffected) but different slopes and *y*-intercepts. Uncompetitive inhibition causes different intercepts on both the *y*- and *x*-axes but the same slope. Mixed inhibitors causes intersect above or below the *x*-axes.

The K_i, values were determined by fitting the kinetic data to a competitive, noncompetitive, or mixed inhibition model by nonlinear regression analysis using GraphPad Prism [51].

4.2.4. Functional activity for cannabinoid receptors on isolated tissue

The functional activity of the new compounds for CB1 receptors was evaluated on the mouse vas deferens preparation. This is a nerve-smooth muscle preparation that serves as a highly sensitive and quantitative functional *in vitro* bioassay for cannabinoid receptor agonists. These ligands induce concentration-related decreases in the amplitude of electrically evoked contractions of the vas deferens by acting on naturally expressed prejunctional neuronal cannabinoid receptors to inhibit release of the contractile neurotransmitters, noradrenaline and ATP, that is provoked by the electrical stimulation [56].

For this study, male ICR mice weighing 25–30 g were used. Mouse vas deferens were isolated as described by Hughes [68]. Tissues were suspended in a 10 mL organ bath containing 5 mL of Krebs solution (NaCl 118; KCl 4.75; $CaCl_2$ 2.54; KH_2PO_4 1.19; $MgSO_4$ 1.2; $NaHCO_3$ 25; glucose 11 mM) that was continuously gassed with 95% O_2 and 5% CO_2. Tissues were kept under 0.5 g of resting tension at 37 °C and were electrically stimulated through two platinum ring electrodes. They were subjected to alternate periods of stimulation (trains of five rectangular pulses of 70 V, 15 Hz and 2 ms duration each were applied every minute) and rest (10 min). The isometric force was monitored by computer using a MacLab data recording and analysis system.

The effect of the synthetic cannabinoid agonist WIN 55,212-2 and that of the new compounds **3**, **5**–**7**, **9**, **12**, **15**, **18**, **23**, and **24**, (10^{-7}–2×10^{-5} M) was tested by constructing concentration–response curves in a step by step manner. Curves were carried out by the following protocol: WIN 55,212-2 or the new compounds were added at a concentration to the organ bath 50 min after the beginning of electrical stimulation and their effect on the electrically induced contractions was evaluated 10 min after their addition. Then, the electrical stimulation was stopped, Krebs solution was replaced and the following concentration of the compound was added. This protocol was repeated for every concentration of the curve.

To test the involvement of the CB1 and CB2 receptors in the effect of the most interesting compounds, they were tested in tissues incubated with the cannabinoid CB1 receptor antagonist AM251 (10^{-6} M) or the combination of both CB1 and CB2 receptor antagonists, AM251 and AM630 (10^{-6} M) respectively. Concentration–response curves for the new compounds were constructed in a step by step manner as follows:

AM251 or the combination of both antagonists was added to the organ bath 50 min after the beginning of electrical stimulation and 10 min later, a dose of WIN 55, 212-2 or the new compounds was added and its effect on the electrically induced contractions was tested 10 min later. Then, the electrical stimulation was stopped, Krebs solution was replaced and this protocol was repeated for every dose of concentration–response curve.

Results have been expressed as % of inhibition, taking the mean amplitude of the last five contractions before the first addition of the agonist as 100%. Each tissue was employed to construct only one concentration–response curve.

Drugs: WIN 55,212-2, AM251 and AM630 were obtained from TOCRIS (Biogen Científica S.L., Madrid, Spain); they were dissolved in ethanol 1 mg:1 mL and subsequently in ethanol and Tween 80 (1:2) after which the ethanol was evaporated [55] and saline solution (0.9%) was added.

The new compounds were dissolved in ethanol, getting a first concentration of 10^{-2} M that was further diluted in distillate water.

4.2.5. Oxygen radical absorbance capacity assay

The ORAC-FL method of Ou et al. [57] partially modified by Dávalos et al. [58] was followed, using a Polarstar Galaxy plate

reader (BMG Labtechnologies GmbH, Offenburg, Germany) with 485-P excitation and 520-P emission filters. The equipment was controlled by Fluorostar Galaxy software (version 4.11-0) for fluorescence measurement. 2,2′-Azobis(amidinopropane) dihydrochloride (AAPH), (±)-6-hydroxy-2,5,7,8-tetramethylchromane-2-carboxylic acid (Trolox), and fluorescein (FL) were purchased from Sigma–Aldrich. The reaction was carried out in 75 mM phosphate buffer (pH 7.4), and the final reaction mixture was 200 μL. Antioxidant (20 μL) and FL (120 μL, 70 mM, final concentration) solutions were placed in a black 96-well microplate (96F untreat, Nunc). The mixture was preincubated for 15 min at 37 °C, and then AAPH solution (60 μL, 12 mM, final concentration) was added rapidly using a multichannel pipette. The microplate was immediately placed in the reader and the fluorescence recorded every minute for 80 min. The microplate was automatically shaken prior each reading. Samples were measured at eight different concentrations (0.1–1 μM). A blank (FL + AAPH in phosphate buffer) instead of the sample solution and eight calibration solutions using Trolox (1–8 μM) were also used in each assay. All the reaction mixtures were prepared in duplicate, and at least three independent assays were performed for each sample. Raw data were exported from the Fluostar Galaxy software to an Excel sheet for further calculations. Antioxidant curves (fluorescence vs time) were first normalized to the curve of the blank corresponding to the same assay, and the area under the fluorescence decay curve (AUC) was calculated. The net AUC corresponding to a sample was calculated by subtracting the AUC corresponding to the blank. Regression equations between net AUC and antioxidant concentration were calculated for all samples. ORAC-FL values were expressed as Trolox equivalents by using the standard curve calculated for each assay, where the ORAC-FL value of Trolox was taken as 1.

4.3. Docking studies

All calculations were performed using the SYBYL 8.1 program suite [Tripos Inc., St. Louis. Mo 1]. The docking studies were achieved using the FlexiDock module of the SYBYL 8.1 suite of programs.

The structures of the ligands were built with standard bond lengths and angles using the molecular modelling package SYBYL 8.1 and their energies were minimized using the conjugate gradient algorithm with a conjugated gradient of <0.001 kcal/mol convergent criteria provided by the MMFF94 force field [69,70] and MMFF94 electrostatic charges.

The structure of AChE and BuChE (pdb code: 1B14 and 1P0I) were edited, protein hydrogen atoms were added and partial charges were calculated using AMBER procedure. Positions of the hydrogen atoms were refined with the use of AMBER force field.

The ligands were placed manually in the gorge limited by PAS and CAS in AChE and BuChE. The ligand–receptor complex was subjected to energy minimization using the MMFF94 force field and MMFF94 electrostatic charges and their energies were minimized using the protocol previously indicated with a conjugate gradient of <0.1 kcal/mol convergent criteria. A distance-dependent dielectric constant was used in all the calculations. These complexes were the input structure for docking using FlexiDock command. During the flexible docking analysis, the ligands and a sphere of 6Å around the corresponding ligand were considered flexibles. For each complex three flexible docking analysis were run. The default FlexiDock parameters were utilized in all cases, with maximum and minimum iterations (MI) set for each complex according to MI = [No. of rotatable bonds in the protein + No. of rotatable bonds in the ligand + 6 × 1000 − 500, obtaining a series of model complexes.

The conformations were analyzed in terms of interactions between ligand and the known key residues. We choose the conformation with highest FlexiDock score (better interactions) and refine the minimization energy step using a conjugate gradient of <0.01 kcal/mol convergent criteria. Analysis of the refined receptor–ligand complex models was based on hydrogen bond, aromatic and hydrophobic interactions predicted with the LPC program [71] and the values of ΔG binding and dissociation constants obtained from the difference accessible surface area method using the STC program [65].

Acknowledgements

The authors gratefully acknowledge the financial support of Spanish Ministry of Science and Innovation (project CTQ2009-07664) and from “Comunidad de Madrid, Programa de Biociencias” (S-SAL-0261/2006) and would like to thank to Guadalupe Pablo for her excellent technical assistance.

Appendix A. Supplementary data

Supplementary data related to this article can be found at http://dx.doi.org/10.1016/j.ejmech.2013.11.026.

References

[1] J.A. Claassen, R.W. Jansen, Cholinergically mediated augmentation of cerebral perfusion in Alzheimer's disease and related cognitive disorders: the cholinergic-vascular hypothesis, J. Gerontol. A Biol. Sci. Med. Sci. 61 (2006) 267–271.
[2] E. Coulthard, V. Singh-Curry, M. Husain, Treatment of attention deficits in neurological disorders, Curr. Opin. Neurol. 19 (2006) 613–618.
[3] M. Villarroya, A.G. Garcia, J. Marco-Contelles, M.G. Lopez, An update on the pharmacology of galantamine, Expert Opin. Investig. Drugs 16 (2007) 1987–1998.
[4] H.W. Klafki, M. Staufenbiel, J. Kornhuber, J. Wiltfang, Therapeutic approaches to Alzheimer's disease, Brain 129 (2006) 2840–2855.
[5] M.A. Kamal, X. Qu, Q.S. Yu, D. Tweedie, H.W. Holloway, Y. Li, Y. Tan, N.H. Greig, Tetrahydrofurobenzofuran cymserine, a potent butyrylcholinesterase inhibitor and experimental Alzheimer drug candidate, enzyme kinetic analysis, J. Neural Transm. 115 (2008) 889–898.
[6] R.M. Lane, S.G. Potkin, A. Enz, Targeting acetylcholinesterase and butyrylcholinesterase in dementia, Int. J. Neuropsychopharmacol. 9 (2006) 101–124.
[7] R. Annicchiarico, A. Federici, C. Pettenati, C. Caltagirone, Rivastigmine in Alzheimer's disease: cognitive function and quality of life, Ther. Clin. Risk Manag. 3 (2007) 1113–1123.
[8] R. Bullock, R. Lane, Executive dyscontrol in dementia, with emphasis on subcortical pathology and the role of butyrylcholinesterase, Curr. Alzheimer Res. 4 (2007) 277–293.
[9] A. Castro, A. Martinez, Peripheral and dual binding site acetylcholinesterase inhibitors: implications in treatment of Alzheimer's disease, Mini Rev. Med. Chem. 1 (2001) 267–272.
[10] G.V. De Ferrari, M.A. Canales, I. Shin, L.M. Weiner, I. Silman, N.C. Inestrosa, A structural motif of acetylcholinesterase that promotes amyloid beta-peptide fibril formation, Biochemistry 40 (2001) 10447–10457.
[11] N.C. Inestrosa, A. Alvarez, M.C. Dinamarca, T. Perez-Acle, M. Colombres, Acetylcholinesterase-amyloid-beta-peptide interaction: effect of Congo Red and the role of the Wnt pathway, Curr. Alzheimer Res. 2 (2005) 301–306.
[12] P. Masson, M.T. Froment, C.F. Bartels, O. Lockridge, Asp7O in the peripheral anionic site of human butyrylcholinesterase, Eur. J. Biochem. 235 (1996) 36–48.
[13] P. Masson, W. Xie, M.T. Froment, V. Levitsky, P.L. Fortier, C. Albaret, O. Lockridge, Interaction between the peripheral site residues of human butyrylcholinesterase, D70 and Y332, in binding and hydrolysis of substrates, Biochim. Biophys. Acta 1433 (1999) 281–293.
[14] S. Diamant, E. Podoly, A. Friedler, H. Ligumsky, O. Livnah, H. Soreq, Butyrylcholinesterase attenuates amyloid fibril formation in vitro, Proc. Natl. Acad. Sci. U. S. A. 103 (2006) 8628–8633.
[15] N.H. Greig, T. Utsuki, D.K. Ingram, Y. Wang, G. Pepeu, C. Scali, Q.S. Yu, J. Mamczarz, H.W. Holloway, T. Giordano, D. Chen, K. Furukawa, K. Sambamurti, A. Brossi, D.K. Lahiri, Selective butyrylcholinesterase inhibition elevates brain acetylcholine, augments learning and lowers Alzheimer beta-amyloid peptide in rodent, Proc. Natl. Acad. Sci. U. S. A. 102 (2005) 17213–17218.
[16] M. Bajda, N. Guzior, M. Ignasik, B. Malawska, Multi-target-directed ligands in Alzheimer's disease treatment, Curr. Med. Chem. 18 (2011) 4949–4975.

[17] Y. Rook, K.U. Schmidtke, F. Gaube, D. Schepmann, B. Wunsch, J. Heilmann, J. Lehmann, T. Winckler, Bivalent beta-carbolines as potential multitarget anti-Alzheimer agents, J. Med. Chem. 53 (2010) 3611–3617.
[18] M. Incerti, L. Flammini, F. Saccani, G. Morini, M. Comini, M. Coruzzi, E. Barocelli, V. Ballabeni, S. Bertoni, Dual-acting drugs: an in vitro study of nonimidazole histamine H3 receptor antagonists combining anticholinesterase activity, ChemMedChem 5 (2010) 1143–1149.
[19] L. Piazzi, A. Cavalli, F. Colizzi, F. Belluti, M. Bartolini, F. Mancini, M. Recanatini, V. Andrisano, A. Rampa, Multi-target-directed coumarin derivatives: hAChE and BACE1 inhibitors as potential anti-Alzheimer compounds, Bioorg. Med. Chem. Lett. 18 (2008) 423–426.
[20] W. Huang, D. Lv, H. Yu, R. Sheng, S.C. Kim, P. Wu, K. Luo, J. Li, Y. Hu, Dual-target-directed 1,3-diphenylurea derivatives: BACE 1 inhibitor and metal chelator against Alzheimer's disease, Bioorg. Med. Chem. 18 (2010) 5610–5615.
[21] M. Hieke, J. Ness, R. Steri, M. Dittrich, C. Greiner, O. Werz, K. Baumann, M. Schubert-Zsilavecz, S. Weggen, H. Zettl, Design, synthesis, and biological evaluation of a novel class of gamma-secretase modulators with PPARgamma activity, J. Med. Chem. 53 (2010) 4691–4700.
[22] J.H. Lange, H.K. Coolen, M.A. van der Neut, A.J. Borst, B. Stork, P.C. Verveer, C.G. Kruse, Design, synthesis, biological properties, and molecular modeling investigations of novel tacrine derivatives with a combination of acetylcholinesterase inhibition and cannabinoid CB1 receptor antagonism, J. Med. Chem. 53 (2010) 1338–1346.
[23] N.E. Campillo, J.A. Paez, Cannabinoid system in neurodegeneration: new perspectives in Alzheimer's disease, Mini Rev. Med. Chem. 9 (2009) 539–559.
[24] S.H. Walter, M. Halpern, Cannabinoids and dementia: review of clinical and preclinical data, Pharmaceuticals 3 (2010) 2689–2708.
[25] B.G. Ramirez, C. Blazquez, T. Gomez del Pulgar, M. Guzman, M.L. de Ceballos, Prevention of Alzheimer's disease pathology by cannabinoids: neuroprotection mediated by blockade of microglial activation, J. Neurosci. 25 (2005) 1904–1913.
[26] J.H. Lee, G. Agacinski, J.H. Williams, G.K. Wilcock, M.M. Esiri, P.T. Francis, P.T. Wong, C.P. Chen, M.K. Lai, Intact cannabinoid CB1 receptors in the Alzheimer's disease cortex, Neurochem. Int. 57 (2010) 985–989.
[27] S. Kalifa, E.K. Polston, J.S. Allard, K.F. Manaye, Distribution patterns of cannabinoid CB1 receptors in the hippocampus of APPswe/PS1DeltaE9 double transgenic mice, Brain Res. 376 (2011) 94–100.
[28] C. Benito, W.K. Kim, I. Chavarria, C.J. Hillard, K. Mackie, R.M. Tolon, K. Williams, J. Romero, A glial endogenous cannabinoid system is upregulated in the brains of macaques with simian immunodeficiency virus-induced encephalitis, J. Neurosci. 25 (2005) 2530–2536.
[29] C. Benito, E. Nunez, R.M. Tolon, E.J. Carrier, A. Rabano, C.J. Hillard, J. Romero, Cannabinoid CB2 receptors and fatty acid amide hydrolase are selectively overexpressed in neuritic plaque-associated glia in Alzheimer's disease brains, J. Neurosci. 23 (2003) 11136–11141.
[30] C. Benito, R.M. Tolon, M.R. Pazos, E. Nunez, A.I. Castillo, J. Romero, Cannabinoid CB2 receptors in human brain inflammation, Br. J. Pharmacol. 153 (2008) 277–285.
[31] R.M. Tolon, E. Nunez, M.R. Pazos, C. Benito, A.I. Castillo, J.A. Martinez-Orgado, J. Romero, The activation of cannabinoid CB2 receptors stimulates in situ and in vitro beta-amyloid removal by human macrophages, Brain Res. 1283 (2009) 148–154.
[32] J.C. Ashton, M. Glass, The cannabinoid CB2 receptor as a target for inflammation-dependent neurodegeneration, Curr. Neuropharmacol. 5 (2007) 73–80.
[33] Y. Marchalant, F. Cerbai, H.M. Brothers, G.L. Wenk, Cannabinoid receptor stimulation is anti-inflammatory and improves memory in old rats, Neurobiol. Aging 29 (2008) 1894–1901.
[34] V.A. Campbell, A. Gowran, Alzheimer's disease; taking the edge off with cannabinoids? Br. J. Pharmacol. 152 (2007) 655–662.
[35] N.G. Milton, Phosphorylated amyloid-beta: the toxic intermediate in alzheimer's disease neurodegeneration, Subcell. Biochem. 38 (2005) 381–402.
[36] J. Ehrhart, D. Obregon, T. Mori, H. Hou, N. Sun, Y. Bai, T. Klein, F. Fernandez, J. Tan, R.D. Shytle, Stimulation of cannabinoid receptor 2 (CB2) suppresses microglial activation, J. Neuroinflammation 2 (2005) 29.
[37] P. Gonzalez-Naranjo, N.E. Campillo, C. Perez, J.A. Paez, Multitarget cannabinoids as novel strategy for Alzheimer disease, Curr. Alzheimer Res. 10 (2013) 229–239.
[38] J.A. Páez, N.E. Campillo, P. González-Naranjo, C. Pérez, V.J. Arán, M.I. Martin Fontelles, R. Girón, E.M. Sánchez, Preparation of 3-Indazolyl Ethers with Cannabinoid and/or Cholinergic Properties Useful for Treating Various Diseases, Universidad Rey Juan Carlos, Spain, ES 2378139 (Oct. 1, 2009), WO 2011039388 (Sep 30, 2010).
[39] S. Rizzo, A. Tarozzi, M. Bartolini, G. Da Costa, A. Bisi, S. Gobbi, F. Belluti, A. Ligresti, M. Allara, J.P. Monti, V. Andrisano, V. Di Marzo, P. Hrelia, A. Rampa, 2-Arylbenzofuran-based molecules as multipotent Alzheimer's disease modifying agents, Eur. J. Med. Chem. 58 (2012) 519–532.
[40] C. Montero, N.E. Campillo, P. Goya, J.A. Paez, Homology models of the cannabinoid CB1 and CB2 receptors. A docking analysis study, Eur. J. Med. Chem. 40 (2005) 75–83.
[41] K. Pfannstiel, J. Janecke, Representation of o-hydrazino-benzoic acids and indazolones by reduction of diazotated anthranilic acids with sulphuric acid, Chem. Ber. 75 (1942) 1096–1107.
[42] V.J. Arán, M. Flores, P. Munoz, J.A. Paez, P. SanchezVerdu, M. Stud, Analogues of cytostatic, fused indazolinones: synthesis, conformational analysis and cytostatic activity against HeLa cells of some 1-substituted indazolols, 2-substituted indazolinones, and related compounds, Liebigs Ann. (1996) 683–691.
[43] L. Baiocchi, G. Corsi, G. Palazzo, Synthesis, properties and reactions of 1*H*-indazol-3-ols and 1-2-dihydro-3h-indazol-3-ones, Synthesis-Stuttgart (1978) 633–648.
[44] P. Bruneau, C. Delvare, M.P. Edwards, R.M. McMillan, Indazolinones, a new series of redox-active 5-lipoxygenase inhibitors with built-in selectivity and oral activity, J. Med. Chem. 34 (1991) 1028–1036.
[45] M.C. Vega, M. Rolon, A. Montero-Torres, C. Fonseca-Berzal, J.A. Escario, A. Gomez-Barrio, J. Galvez, Y. Marrero-Ponce, V.J. Aran, Synthesis, biological evaluation and chemometric analysis of indazole derivatives. 1,2-Disubstituted 5-nitroindazolinones, new prototypes of antichagasic drug, Eur. J. Med. Chem. 58 (2012) 214–227.
[46] M.R. Lauwiner, R.P. Wissmann, Reduction of aromatic nitro compounds with hydrazine hydrate in the presence of an iron oxide hydroxide catalyst. I. The reduction of monosubstituted nitrobenzenes with hydrazine hydrate in the presence of ferrihydrite, Appl. Catal. A Gen. 172 (1998) 7.
[47] G.L. Ellman, K.D. Courtney, V. Andres Jr., R.M. Feather-Stone, A new and rapid colorimetric determination of acetylcholinesterase activity, Biochem. Pharmacol. 7 (1961) 88–95.
[48] M.L. Bolognesi, M. Bartolini, A. Cavalli, V. Andrisano, M. Rosini, A. Minarini, C. Melchiorre, Design, synthesis, and biological evaluation of conformationally restricted rivastigmine analogues, J. Med. Chem. 47 (2004) 5945–5952.
[49] E. Giacobini, Cholinesterases: new roles in brain function and in Alzheimer's disease, Neurochem. Res. 28 (2003) 515–522.
[50] H.A. Grigoryan, A.A. Hambardzumyan, M.V. Mkrtchyan, V.O. Topuzyan, G.P. Halebyan, R.S. Asatryan, alpha,beta-Dehydrophenylalanine choline esters, a new class of reversible inhibitors of human acetylcholinesterase and butyrylcholinesterase, Chem. Biol. Interact. 171 (2008) 108–116.
[51] GraphPad_Prism, GraphPad Software, San Diego, CA, USA, 2013.
[52] M. Bartolini, C. Bertucci, V. Cavrini, V. Andrisano, beta-Amyloid aggregation induced by human acetylcholinesterase: inhibition studies, Biochem. Pharmacol. 65 (2003) 407–416.
[53] C. Cano, P. Goya, J.A. Paez, R. Giron, E. Sanchez, M.I. Martin, Discovery of 1,1-dioxo-1,2,6-thiadiazine-5-carboxamide derivatives as cannabinoid-like molecules with agonist and antagonist activity, Bioorg. Med. Chem. 15 (2007) 7480–7493.
[54] J. Cumella, L. Hernandez-Folgado, R. Giron, E. Sanchez, P. Morales, D.P. Hurst, M. Gomez-Canas, M. Gomez-Ruiz, D.C. Pinto, P. Goya, P.H. Reggio, M.I. Martin, J. Fernandez-Ruiz, A.M. Silva, N. Jagerovic, Chromenopyrazoles: non-psychoactive and selective CB(1) cannabinoid agonists with peripheral anti-nociceptive properties, ChemMedChem 7 (2012) 452–463.
[55] R.G. Pertwee, L.A. Stevenson, D.B. Elrick, R. Mechoulam, A.D. Corbett, Inhibitory effects of certain enantiomeric cannabinoids in the mouse vas deferens and the myenteric plexus preparation of guinea-pig small intestine, Br. J. Pharmacol. 105 (1992) 980–984.
[56] A. Thomas, R.G. Pertwee, The bioassay of cannabinoids using the mouse isolated vas deferens, Methods Mol. Med. 123 (2006) 191–207.
[57] B. Ou, M. Hampsch-Woodill, R.L. Prior, Development and validation of an improved oxygen radical absorbance capacity assay using fluorescein as the fluorescent probe, J. Agric. Food Chem. 49 (2001) 4619–4626.
[58] A. Davalos, C. Gomez-Cordoves, B. Bartolome, Extending applicability of the oxygen radical absorbance capacity (ORAC-fluorescein) assay, J. Agric. Food. Chem. 52 (2004) 48–54.
[59] SYBYL 7.2, Tripos International, 1699 South Hanley Rd., St. Louis, Missouri, 63144, USA.
[60] J. Ramos, V.L. Cruz, J. Martinez-Salazar, N.E. Campillo, J.A. Paez, Dissimilar interaction of CB1/CB2 with lipid bilayers as revealed by molecular dynamics simulation, Phys. Chem. Chem. Phys. 13 (2011) 3660–3668.
[61] K. Palczewski, T. Kumasaka, T. Hori, C.A. Behnke, H. Motoshima, B.A. Fox, I. Le Trong, D.C. Teller, T. Okada, R.E. Stenkamp, M. Yamamoto, M. Miyano, Crystal structure of rhodopsin: a G protein-coupled receptor, Science 289 (2000) 739–745.
[62] A. Poso, J.W. Huffman, Targeting the cannabinoid CB2 receptor: modelling and structural determinants of CB2 selective ligands, Br. J. Pharmacol. 153 (2008) 335–346.
[63] G. Kryger, M. Harel, K. Giles, L. Toker, B. Velan, A. Lazar, C. Kronman, D. Barak, N. Ariel, A. Shafferman, I. Silman, J.L. Sussman, Structures of recombinant native and E202Q mutant human acetylcholinesterase complexed with the snake-venom toxin fasciculin-II, Acta Crystallogr. D Biol. Crystallogr. 56 (2000) 1385–1394.
[64] Y. Nicolet, O. Lockridge, P. Masson, J.C. Fontecilla-Camps, F. Nachon, Crystal structure of human butyrylcholinesterase and of its complexes with substrate and products, J. Biol. Chem. 278 (2003) 41141–41147.
[65] P. Lavigne, J.R. Bagu, R. Boyko, L. Willard, C.F. Holmes, B.D. Sykes, Structure-based thermodynamic analysis of the dissociation of protein phosphatase-1 catalytic subunit and microcystin-LR docked complexes, Protein Sci. 9 (2000) 252–264.
[66] Y. Cheng, W.H. Prusoff, Relationship between the inhibition constant (K1) and the concentration of inhibitor which causes 50 per cent inhibition (I50) of an enzymatic reaction, Biochem. Pharmacol. 22 (1973) 3099–3108.

[67] G. Griffin, Q. Tao, M.E. Abood, Cloning and pharmacological characterization of the rat CB(2) cannabinoid receptor, J. Pharmacol. Exp. Ther. 292 (2000) 886–894.
[68] J. Hughes, H.W. Kosterlitz, F.M. Leslie, Effect of morphine on adrenergic transmission in the mouse vas deferens. Assessment of agonist and antogonist potencies of narcotic analgesics, Br. J. Pharmacol. 53 (1975) 371–381.
[69] P.A. Halgren, Merck molecular force field. I. Basis, form, scope, parameterization, and performance of MMFF94, J. Comput. Chem. 17 (1996) 450–519.
[70] P.A. Halgren, Merck molecular force field. 2. MMFF94 van der Waals and electrostatic parameters for intermolecular interactions, J. Comput. Chem. 17 (1996) 520–552.
[71] V. Sobolev, A. Sorokine, J. Prilusky, E.E. Abola, M. Edelman, Automated analysis of interatomic contacts in proteins, Bioinformatics 15 (1999) 327–332.